

RECEIVED: January 13, 2022

REVISED: April 8, 2022

ACCEPTED: April 12, 2022

PUBLISHED: May 3, 2022

# Nuclei in the toy world: beyond the Pomeron in zero transverse dimensions

# Alex Kovner,a,b Eugene Levinb,c and Michael Lublinskyd

- <sup>a</sup> Physics Department, University of Connecticut, 2152 Hillside Road, Storrs, CT 06269, U.S.A.
- <sup>b</sup>Department of Particle Physics, Tel Aviv University, Tel Aviv 69978, Israel
- Contra Departemento de Física, Universidad Técnica Federico Santa María and Centro Científico-Tecnológico de Valparaíso,
   Avda. Espana 1680, Casilla 110-V, Valparaíso, Chile
- <sup>d</sup>Physics Department, Ben-Gurion University of the Negev, Beer Sheva 84105, Israel

E-mail: alexander.kovner@uconn.edu, leving@tauex.tau.ac.il, lublinm@bgu.ac.il

ABSTRACT: We explore possible extensions of the t-channel and s-channel unitary model of high energy evolution in zero transverse dimensions appropriate to very high energy/atomic number where the dipole density in a toy hadron is parametrically high. We suggest that the appropriate generalization is to allow emission of more than one dipole in a single step of energy evolution. We construct explicitly such a model that preserves the t-channel and s-channel unitarity and have the correct low density limit, and study the particle multiplicity distribution resulting from this evolution. We consider initial conditions of a single dipole and many dipoles at initial rapidity. We observe that the saturation regime in this model is preceded by a parametric range of rapidities  $\frac{1}{\alpha_s} \ln \frac{1}{\alpha_s} < Y < \frac{1}{\alpha_s} \ln \frac{1}{\alpha_s^2}$ , where the saturation effects are still unimportant, but multiple emissions determine the properties of the evolution. We also discuss the influence of the saturation on the parton cascade and, in particular, find that in the saturation regime the entropy of partons becomes  $S \approx \frac{1}{2} \ln N$  where N is the mean multiplicity.

KEYWORDS: Deep Inelastic Scattering or Small-X Physics, Effective Field Theories of QCD, Quark-Gluon Plasma, Resummation

ArXiv ePrint: 2201.01551

1	Intr	roduction	1
2	The	e unitary toy model (UTM)	3
	2.1	The RFT formulation	3
	2.2	The frame invariant formulation	6
	2.3	The BFKL-BK limit	7
	2.4	The UTM probability distribution	8
		2.4.1 The asymptotic distribution at $Y \to \infty$	8
		2.4.2 The UTM parton cascade at "intermediate" $n$	10
3	Ger	neralizing UTM	12
	3.1	Emission of two gluons per one step of evolution	13
	3.2	Emission of infinite number of gluons in one step of evolution	15
		3.2.1 Multiple emissions without saturation $(\frac{1}{\Delta} < n < \frac{1}{\gamma})$	16
		3.2.2 The S-matrix for single and multiple gluon emissions	19
		3.2.3 Multiple emissions with saturation — large Y asymptotics $(n \gg \frac{1}{\gamma})$	22
4	"Nı	m and evolution: the $m$ -dipole initial condition	24
	4.1	Many dipoles evolved with BK	25
	4.2	m-dipoles in UTM at intermediate rapidities	26
	4.3	UTM at asymptotically large rapidities	26
	4.4	UTMM — multiple emissions without saturation	27
	4.5	UTMM with saturation	29
5	Dis	cussion	30
A	Fac	torial moments and probabilities in UTMM	33

#### 1 Introduction

The question of asymptotic behavior of hadronic scattering amplitude at high energy has been actively studied over many decades. It is well understood by now that at high enough energy the fast growth of the scattering amplitude slows down and that the physical phenomenon that is responsible for it, is the saturation of partons in hadronic wave function. The quantitative description of this saturation however is a difficult question. We believe that the appropriate framework is the so called Reggeon Field Theory (RFT) where the effective degrees of freedom are scattering amplitude and the evolution parameter is the logarithm of energy (rapidity) [1–34]. Currently we know how to construct the evolution of the

amplitudes and the hadronic wave function appropriate for the situation when one of the colliding hadrons may be dense, but the other one remains dilute at the energy of interest.

Once the energy grows even further so that both hadrons have to be considered dense nontrivial modification of the current theory is necessary. This also pertains to collision of heavy ions at lower energies, where the partonic density is large already at get go. Much thought has gone into attempting to extend the current theory to this regime [35–50], but a consistent description of the dense regime is still wanting.

Although a proper QCD derivation of the high energy RFT is not available, there are several constraints on the eventual form of this theory that follow from fundamental unitarity requirements. In particular, the effective theory should be s-channel unitary and t-channel unitary.

The t-channel unitarity condition can be formulated in different ways. One way of putting it is the requirement that the scattering amplitude does not depend on the frame in which the scattering is described. Mathematically this is equivalent to the property of self-duality of the RFT [58]. This property is built in the BFKL evolution [1–4] which is appropriate for the scattering of two dilute objects. It is however lacking in the BK or JIMWLK equations [33, 34, 51–57], which describe the scattering of a dilute object on a dense one. Recently we have proposed a generalization of JIMWLK evolution which does preserve the t-channel unitarity [59, 60].

The s-channel unitarity has only been discussed recently in this context. It does not have a simple mathematical formulation, but physically is equivalent to the requirement that RFT is derivable from a fundamental unitary quantum field theory. The s-channel unitarity turns out to be a difficult constraint to satisfy. Neither BFKL nor JIMWLK evolution satisfy it fully, and it has not been established so far in any of the putative generalizations [59].

An interesting question to ask is whether imposing the two unitarity conditions is restrictive enough to determine the RFT completely. Or perhaps better to say, what additional guidance about RFT one can obtain from physical considerations beyond unitarity.

While the quantitative theory of course should be derived directly from QCD, over the years we have found simple toy models to be quite illuminating. Thus much work in early days was done on models with zero transverse dimensions in an attempt to understand general features of Pomeron interactions [8, 9, 61–73]. Later similar zero dimensional models have been studied as a good playground to explore general features which must be present in the effective high energy theory of QCD. These universal features include t-channel unitarity and s-channel unitarity. Recently we have suggested a simple zero dimensional model which satisfies both unitarity conditions [74].

In this paper we further study zero dimensional case. In section 2 we discuss the relation of the model of [74] with a t-channel unitary model introduced in [23] and later in [75] and studied in detail in [71]. We show that the two models lead to identical evolution equations for the dipole probabilities, and are therefore equivalent. Below we will refer to this model UTM — unitary toy model. We also show that the generating function frequently introduced in the framework of dipole evolution, in the RFT formulation of the same theory plays the role of the Schroedinger wave function.

In section 3 we point out that the RFT formulation is rather flexible and allows to generalize the model in question in a way that preserves the correct unitarity properties. The new physical ingredient that enters this generalization is the observation that in one step of the evolution the emission does not have to be limited to just one gluon. In fact we argue that in the high energy dense regime one should expect emission of any number of gluons with appropriate probabilities. While in the dilute limit the emission of the additional gluons is suppressed by powers of the coupling constant, thus corresponding to NLO corrections to the emission kernel, this is not the case in the asymptotic dense regime. We construct explicitly an RFT Hamiltonian (below referred to as UTMM), which implements such an evolution and study some of its properties. In particular we observe that it leads to a much wider distribution of dipoles in the wave function at high energy compared to the original toy model. In both sections 2 and 3 we study the saturation effects in the parton cascades which are not included in the JIMWLK(BK) approach. The effect of saturation are physically the same as summation of the BFKL Pomeron loops, albeit the language we use in this paper is different. This problem has not been solved in QCD, hence the experience with the exact solvable simplified models could be useful.

Sections 2 and 3 focus on dipole evolution of a single dipole taken as initial condition. In section 4 we explore the effect of initial conditions on the probability distribution. In particular we solve for the probability distributions in UTM and UTMM but for m dipoles in the wave function as initial condition. We show that, as expected, increasing m shifts the asymptotic regime to lower rapidities. In particular if the initial number of dipoles is very large  $m \sim 1/\gamma$ , where  $\gamma$  it the dipole-dipole scattering amplitude, the BK regime is absent in the evolution and the saturation regime dominates from the get go.

Finally section 5 is devoted to discussion of several qualitative features of the models we consider.

#### 2 The unitary toy model (UTM)

# 2.1 The RFT formulation

In [74] we have discussed the zero dimensional toy model defined as an RFT. Mathematically the setup is the following. The projectile and target states of RFT are defined by the action of (projectile and target) dipole operators d and  $\bar{d}$  on the left and right vacua respectively. The general RFT "wave function" of the target at rapidity  $Y^T$  has the form

$$|\Psi_T\rangle_{Y^T} = \sum_n P_n^T(Y^T)\bar{d}^n|0\rangle \tag{2.1}$$

where  $P_n^T(Y^T)$  are probabilities to have n dipoles in the target state,  $P_n^T \ge 0$ ,  $\sum_n P_n^T = 1$ . Similarly for the projectile the most general state is

$$\langle \Psi_P | = \sum_m P_m^P(Y^P) \langle 0 | d^m$$
 (2.2)

Note that although we refer to the above objects as "wave functions", those are not wave functions of any quantum theory, but rather "wave functions" of RFT. As such their

physical meaning is different from the usual Schroedinger wave functions. In particular the coefficients in their expansion in the dipole basis are themselves physical probabilities, rather than amplitudes whose squares yield probabilities in the standard quantum mechanical setting.

In terms of these objects the scattering amplitude is calculated as

$$s = \langle \Psi_P(d) | \Psi_T(\bar{d}) \rangle \tag{2.3}$$

To calculate the overlap we use the algebra of the dipole operators

$$d\bar{d} = e^{-\gamma} \bar{d}d; \tag{2.4}$$

and the properties of the right and left "vacua"

$$d|0\rangle = 0; \qquad \langle 0|\bar{d} = 0 \tag{2.5}$$

The constant  $e^{-\gamma}$  has the meaning of a dipole-dipole scattering matrix. In the following we assume the scattering to be weak, so that in the natural counting in powers of the coupling constant  $\gamma \sim \alpha_s^2$ . This is consistent with the scattering amplitude of two dipoles in QCD. With the assumption that  $\gamma$  is small, and will freely use  $e^{-\gamma} \approx 1 - \gamma$  whenever convenient.

Note that the algebra of d and  $\bar{d}$  can be represented explicitly on functions of  $\bar{d}$  by 1

$$d = \exp\{-\gamma \bar{d} \frac{\partial}{\partial \bar{d}}\}\tag{2.6}$$

As a consequence

$$\langle 0|d^m \bar{d}^n|0\rangle = e^{-\gamma mn} \tag{2.7}$$

and

$$s(Y) = \sum_{m,n} e^{-\gamma mn} P_m^P(Y_0) P_n^T(Y - Y_0) \equiv \sum_{m,n} \sigma^{mn} P_m^P(Y_0) P_n^T(Y - Y_0)$$
 (2.8)

with  $\sigma = e^{-\gamma}$ . In this expression the total rapidity (logarithm of energy) of the scattering process is Y, while  $Y_0$  defines the frame in which the calculation (observation) is performed. The physical amplitude of course should be independent of  $Y_0$  and depend on Y only.

The energy evolution of the scattering amplitude is given by the evolution equation generated by an RFT Hamiltonian according to

$$s(Y) = \langle \Psi_P(d) | e^{-HY} | \Psi_T(\bar{d}) \rangle \tag{2.9}$$

where H is an operator function of d and  $\bar{d}$ .

The unitarized toy model (UTM) of [74] is defined by the Hamiltonian

$$H_{UTM} = -\frac{\Delta}{\gamma}\bar{P}P\tag{2.10}$$

 $<sup>^{1}</sup>$ We have used the symbol of partial derivative in order to avoid confusion between the differential d and the dipole operator d.

where the Pomeron operators are related to dipoles as

$$P = 1 - d;$$
  $\bar{P} = 1 - \bar{d}.$  (2.11)

The Hamiltonian generates the evolution of the RFT wave function. For a n dipole target state evolved by an infinitesimal rapidity  $\delta Y$ 

$$e^{-H_{UTM}\delta Y}|n\rangle \approx \left(1 - \delta Y \frac{\Delta}{\gamma} \left[1 - e^{-\gamma n}\right]\right)|n\rangle + \delta Y \frac{\Delta}{\gamma} \left[1 - e^{-\gamma n}\right]|n+1\rangle$$
 (2.12)

The constant  $\Delta$  which determines the probability to emit a dipole in one step of the evolution is a model parameter. In terms of the counting of powers of the coupling constant we will set it to be of order  $\Delta \sim \alpha_s$ , which is consistent with QCD. Thus our two model parameters are both small, and  $\gamma \sim \Delta^2$ .

The evolution eq. (2.12) has several important properties. First, it is s-channel unitary. This is obvious since a step in the evolution generates a new dipole state with positive probability. It is also t-channel unitary, as can be seen by explicit derivation of the evolution of a target state, which turns out to be identical to eq. (2.12), [74]. The t-channel unitarity is assured by the self duality of the Hamiltonian. i.e. invariance under the transformation  $d \to \bar{d}$  accompanied by the exchange of order of the factors d and  $\bar{d}$ , which we will refer to as transposition. Explicitly, the duality transformation is

$$H(d, \bar{d}) \to H^T(\bar{d}, d)$$
 (2.13)

Finally, another important point is that the probability of emission of an extra dipole for large n does not depend on n, since  $1 - e^{-\gamma n} \to 1$  for  $n \gg 1/\gamma$ . Thus although for small n (small rapidity) the number of dipoles grows exponentially, at large n the growth is much slower. This feature of saturation is what we expect from the saturation in QCD as well. At large rapidity the cross section is dominated by configurations with large n. Thus the probability to emit an extra dipole is constant and the evolution becomes similar to a random walk in the dipole number space. In this sense the evolution saturates at high energy. We will observe this property explicitly below.

The quantum evolution can be cast in the form of the Schroedinger equation of the RFT. Let us define the target RFT wave function in the  $\bar{d}$  representation(an identical discussion holds for the projectile), i.e.

$$|\Psi\rangle = Z(\bar{d})|0\rangle \tag{2.14}$$

The proper normalization of the RFT wave function is not given by the usual integral condition as for a Schroedinger wave function, but rather by

$$Z(1) = 1 (2.15)$$

The Schroedinger equation for Z is derived by acting with the Hamiltonian eq. (2.10) while utilizing the algebra eq. (2.4) and eq. (2.6):

$$\frac{\partial}{\partial Y} Z_Y^{\text{UTM}}(u) = -\frac{\Delta}{\gamma} (1 - u) \left( 1 - e^{-\gamma u} \frac{\partial}{\partial u} \right) Z_Y^{\text{UTM}}(u) = \frac{\Delta}{\gamma} (u - 1) \left( Z_Y^{\text{UTM}}(u) - Z_Y^{\text{UTM}} \left( e^{-\gamma} u \right) \right)$$
(2.16)

Note that Z is precisely the probability generating function as it is frequently defined in the framework of similar reaction-diffusion models. The standard definition of the generating function is

$$Z_Y(u) \equiv \sum_n P_n(Y)u^n \tag{2.17}$$

so that

$$P_n(Y) = \frac{1}{n!} \frac{\partial^n}{\partial u^n} Z(Y)|_{u=0}$$
(2.18)

Comparing this definition with eq. (2.14) and using eq. (2.1) we see that the two functions are indeed identical.

We note that sometimes rather than calculating probabilities  $P_n^{\text{UTM}}$  it is more useful to calculate factorial moments of the probability distribution defined as

$$M_k \equiv \langle n(n-1)\dots(n-k+1)\rangle \equiv \sum_{n=0}^{\infty} n(n-1)\dots(n-k+1)P_n = \sum_{n=0}^{\infty} \frac{n!}{(n-k)!} P_n$$
 (2.19)

These moments can be calculated from the generating function Z as

$$M_k = \frac{\partial^k}{\partial u^k} Z(u)|_{u=1} \tag{2.20}$$

which is equivalent to the representation

$$Z_Y(u) = 1 + \sum_{k=1}^{\infty} \frac{1}{k!} M_k(Y) (u-1)^k$$
(2.21)

# 2.2 The frame invariant formulation

An alternative approach to defining dipole models of this type was discussed a while ago in [23], and later in [75] and [71]. The starting point of these works is explicit invariance of the evolution equation for probabilities  $P_n$  under the change of Lorentz frame.

One starts with the eq. (2.8) and requires that the evolution of the probabilities is such that the expression for the s-matrix does not depend on the frame in which it is calculated, i.e. on the value of  $Y_0$ . If in addition one assumes that only one dipole is emitted in one step of the evolution, i.e.

$$\frac{d}{dY}P_n(Y) = f_n P_n(Y) + g_n P_{n-1}(Y)$$
 (2.22)

one finds that the only solution compatible with the dilute limit is

$$\frac{dP_n^{\text{UTM}}(Y)}{dY} = -\frac{\Delta}{\gamma} \left( 1 - e^{-\gamma n} \right) P_n^{\text{UTM}}(Y) + \frac{\Delta}{\gamma} \left( 1 - e^{-\gamma (n-1)} \right) P_{n-1}^{\text{UTM}}(Y)$$
 (2.23)

Both models, eq. (2.10) and eq. (2.23) describe the evolution of the same system — an ensemble of dipoles (colorless "partons"). In fact, although it was not realized in [74], the two are equivalent. To see this we should recast the evolution of the RFT wave function in terms of the evolution of probabilities. Starting with eq. (2.12) and reinterpreting it as evolution of probabilities we indeed immediately obtain eq. (2.23). Another way to see this

equivalence is to start with the probability evolution eq. (2.23) and derive the evolution of the generating function defined as eq. (2.17). This equation is identical with eq. (2.16) which again demonstrates that the two models are identical.

It is interesting to understand the main properties of the probability distribution as it evolves from lower to higher rapidities. We will do that in the rest of this section. We note that some of these results have already appeared before, e.g. in [71]. We present them here for completeness, as well as to set up the stage for generalizing the model in the next section.

#### 2.3 The BFKL-BK limit

When one of the colliding objects is dilute, the model above reduces to the zero dimensional BK model. For dilute target, for example the scattering amplitude of each projectile dipole is small, and one can formally expand d in power series in  $\gamma$ 

$$d \approx 1 - \gamma \bar{d} \frac{\partial}{\partial \bar{d}} \tag{2.24}$$

The Hamiltonian then becomes

$$H_{BK} = \Delta \left[ \bar{d}^2 - \bar{d} \right] \frac{\partial}{\partial \bar{d}} \tag{2.25}$$

which is precisely the BK Hamiltonian.

Analysis of this limit is quite straightforward if we restrict ourselves to the properties of the dilute object. As was explained in [74], the BK Hamiltonian violates s-channel unitarity if applied to the wave function of the dense projectile, and we are not going to consider this case. On the other hand when evolving the state of the dilute target the BK evolution of the wave function is equivalent to the BFKL cascade. With this in mind we will allow ourselves to refer to the resulting probability distribution interchangeably as either BK or BFKL.

First off, it is easy to see that the Schoedinger equation becomes

$$\frac{\partial}{\partial Y} Z_Y^{BK}(u) = -\Delta u (1 - u) \frac{\partial}{\partial u} Z_Y^{BK}(u)$$
 (2.26)

This is easily solved noting that it can be rewritten in a simple way as

$$\left[\frac{\partial}{\partial Y} - \frac{\partial}{\partial t}\right] Z^{BK} = 0 \tag{2.27}$$

where

$$t = \frac{1}{\Delta} \ln \frac{1 - u}{u} \tag{2.28}$$

Thus for any initial condition  $Z_0^{BK}(u)$  the solution is

$$Z_Y^{BK}(u) = Z_0^{BK} \left( \frac{u}{u(1 - e^{\Delta Y}) + e^{\Delta Y}} \right)$$
 (2.29)

The most common case considered in the literature is when at initial energy the target contains one single dipole,  $Z_0^{BK} = u$ . In this and the next section we will concentrate on

solutions that correspond to this initial condition. We will consider the case of multiple dipoles at initial rapidity in section 4.

For a single dipole initial condition the solution at rapidity Y is

$$Z_Y^{BK}(u;1) = \frac{u}{u(1 - e^{\Delta Y}) + e^{\Delta Y}}$$
 (2.30)

Using this generating function it is easy to see that (here the index (1) indicates the number of dipoles at initial rapidity)

$$M_{1(1)}^{BK}(Y) \equiv N(Y) = e^{\Delta Y}$$
 (2.31)

and

$$P_{n(1)}^{BK}(Y) = \frac{1}{N(Y) - 1} \left( 1 - \frac{1}{N(Y)} \right)^n \tag{2.32}$$

The higher factorial moments for this distribution have a simple structure:

$$M_{k(1)}^{BK}(Y) = k! N(Y) (N(Y) - 1)^{k-1}$$
 (2.33)

At high energy where  $e^{\Delta Y} \gg 1$  these become

$$P_{n(1)}^{BK}(Y) \to \frac{1}{N(Y)} e^{-\frac{n}{N(Y)}}; \qquad M_{k(1)}^{BK}(Y) \to k! N^k(Y)$$
 (2.34)

# 2.4 The UTM probability distribution

We now turn to the probability distribution in UTM beyond the BFKL-BK limit. Various properties of UTM were studied in depth in [71]. We mention that the equation for probabilities can be explicitly solved. In particular for the initial condition of a single dipole  $P_1(0) = 1$ ;  $P_{n\neq 1}(0) = 0$  the solution is

$$P_{1}^{\text{UTM}}(Y) = e^{-\omega_{1}Y};$$

$$P_{n>1}^{\text{UTM}}(Y) = \oint \frac{d\omega}{2\pi i} e^{\omega Y} \frac{1}{\omega_{n}} \prod_{k=1}^{n} \frac{\omega_{k}}{\omega + \omega_{k}} = \prod_{j=1}^{n-1} \omega_{j} \sum_{i=1}^{n} \prod_{k \neq i, k=1}^{n} \frac{1}{\omega_{k} - \omega_{i}} e^{-\omega_{i}Y}$$
 (2.35)

with

$$\omega_n = \frac{\Delta}{\gamma} [1 - e^{-\gamma n}] \tag{2.36}$$

Although these formulae are explicit, they do not give one directly an understanding of the properties of the distribution. To get a better idea about the importance of the saturation corrections we first consider the limit of very large energy.

#### 2.4.1 The asymptotic distribution at $Y \to \infty$

To find the behavior of the probabilities at high energy we note that for large Y we expect  $Z_Y(e^{-\gamma}u) \ll Z_Y(u)$ , since on average the number of dipoles is expected to be large, which means that high powers of u are most important in the generating function. Thus

to find the large Y asymptotics we can drop the second term in the Schroedinger equation eq. (2.16). The resulting equation is simple

$$\frac{\partial}{\partial Y} Z_Y^{\text{UTM}}(u) = \frac{\Delta}{\gamma} (u - 1) Z_Y^{\text{UTM}}(u)$$
 (2.37)

and yields the asymptotic solution

$$Z_Y^{\text{asymp}}(u) = e^{\frac{\Delta}{\gamma}(u-1)(Y-Y_0)} Z_{Y_0}(u)$$
 (2.38)

Here  $Y_0$  is the rapidity starting from which we can use the asymptotic equation, and the function  $Z_{Y_0}(u)$  is determined by the initial condition and the evolution up to the rapidity  $Y_0$ . For very large rapidity  $Y \gg Y_0$  the exact value of  $Y_0$  does not matter. Likewise the initial condition should not significantly affect the properties of the distribution. Formally we assume that the function  $Z_{Y_0}(u)$  describes states with relatively small number of particles. It therefore is dominated by small powers of u and is a relatively smooth function which can be approximated by a constant. The normalization eq. (2.15) then sets this constant to unity. Thus the asymptotic generating function can be approximated by

$$Z_V^{\text{asymp UTM}}(u) \approx e^{\frac{\Delta}{\gamma}(u-1)Y}$$
 (2.39)

Calculating the probabilities we find the Poisson distribution:

$$P_n^{\text{asymp UTM}} = P_n^{PD}(N) = \frac{N^n(Y)}{n!} e^{-N(Y)}$$
 (2.40)

with the average multiplicity

$$N(Y) = \frac{\Delta}{\gamma} Y \tag{2.41}$$

This distribution can also be directly obtained from the general solution of eq. (2.35) replacing  $\omega_n \to \frac{\Delta}{\gamma}$  which is appropriate for n large such that  $n\gamma \gg 1$ .

The factorial moments for the Poisson distribution are

$$M_k^{PD}(Y) = N^k(Y) \tag{2.42}$$

We note that the properties of this probability distribution are significantly different from that in the BFKL cascade. The average number of dipole grows only linearly with rapidity rather than exponentially. This is a direct consequence of saturation of the emission amplitudes in eq. (2.12) at large n. As noted above, the probability for emission of an extra dipole at large rapidity is a constant and does not depend on the number of dipoles already present in the wave function. As a result the evolution is similar to random walk and the average number of dipoles grows only linearly in rapidity. For BK evolution, where the emission probability is proportional to the number of dipoles present, the growth is exponential as reflected in eq. (2.31). Another important difference is that the distribution eq. (2.40) unlike eq. (2.34) does not obey KNO scaling [76–78] and decreases much faster at large values of n > N(Y) compared to  $P^{BK}$ .

# 2.4.2 The UTM parton cascade at "intermediate" n

The Poisson distribution derived above is valid at asymptotically large energy. What about the intermediate region, where the number of particles is large enough so that the BK limit is not valid, but the energy is still not asymptotically large? We probe this regime assuming that  $P_n^{\text{UTM}}$  is a smooth function of n, i.e. we replace  $P_{n-1}^{\text{UTM}}(Y)$  in eq. (2.23) by

$$P_{n-1}^{\text{UTM}}(Y) = P_n^{\text{UTM}}(Y) - \frac{\partial P_n^{\text{UTM}}(Y)}{\partial n}$$
 (2.43)

which assumes  $\frac{\partial^2 P_n^{\text{UTM}}(Y)}{\partial n^2} \ll \frac{\partial P_n^{\text{UTM}}(Y)}{\partial n}$ . This assumption will have to be checked a posteriori given the solution. In this approximation eq. (2.23) takes the form

$$\frac{\partial P_n^{\text{UTM}}(Y)}{\partial Y} = -\frac{\Delta}{\gamma} \left( \left( 1 - e^{-\gamma} \right) e^{-(n-1)\gamma} P_n^{\text{UTM}}(Y) + \left( 1 - e^{-(n-1)\gamma} \right) \frac{\partial P_n^{\text{UTM}}(Y)}{\partial n} \right) \tag{2.44}$$

We write the solution in the form  $P_n^{\text{UTM}}(Y) = \hat{P}_n \tilde{P}_n(Y)$ , where  $\hat{P}_n$  is a particular solution of the equation:

$$(1 - e^{-\gamma}) e^{-(n-1)\gamma} \hat{P}_n + (1 - e^{-(n-1)\gamma}) \frac{\partial \hat{P}_n}{\partial n} = 0.$$
 (2.45)

This is solved by<sup>2</sup>

$$\hat{P}_n = \exp\left(-\frac{1 - \exp\left(-\gamma\right)}{\gamma} \ln\left(1 - e^{-(n-1)\gamma}\right)\right) \approx \frac{1}{\left(1 - e^{-(n-1)\gamma}\right)}.$$
 (2.46)

The equation for  $\widetilde{P}_n(Y)$  then becomes:

$$\frac{\partial \widetilde{P}_n(Y)}{\partial Y} = -\frac{\Delta}{\gamma} \left( 1 - e^{-(n-1)\gamma} \right) \frac{\partial \widetilde{P}_n(Y)}{\partial n}. \tag{2.47}$$

The general solution of eq. (2.47) is an arbitrary function of  $(\Delta Y + f(n))$  with f(n) satisfying:

$$\frac{df(n)}{dn} = -\frac{\gamma}{1 - e^{-(n-1)\gamma}} \tag{2.48}$$

or

$$f(n) = -\ln\left(e^{(n-1)\gamma} - 1\right) \tag{2.49}$$

Hence

$$P_n^{\text{UTM}}(Y) = \frac{1}{(1 - e^{-(n-1)\gamma})} F(\zeta(Y, n))$$
 (2.50)

where we have defined

$$\zeta(Y,n) = -\Delta Y + \ln \left( \frac{e^{(n-1)\gamma} - 1}{\gamma} \right). \tag{2.51}$$

<sup>&</sup>lt;sup>2</sup>We approximate  $\exp\{-\gamma\} \approx 1 - \gamma$ .

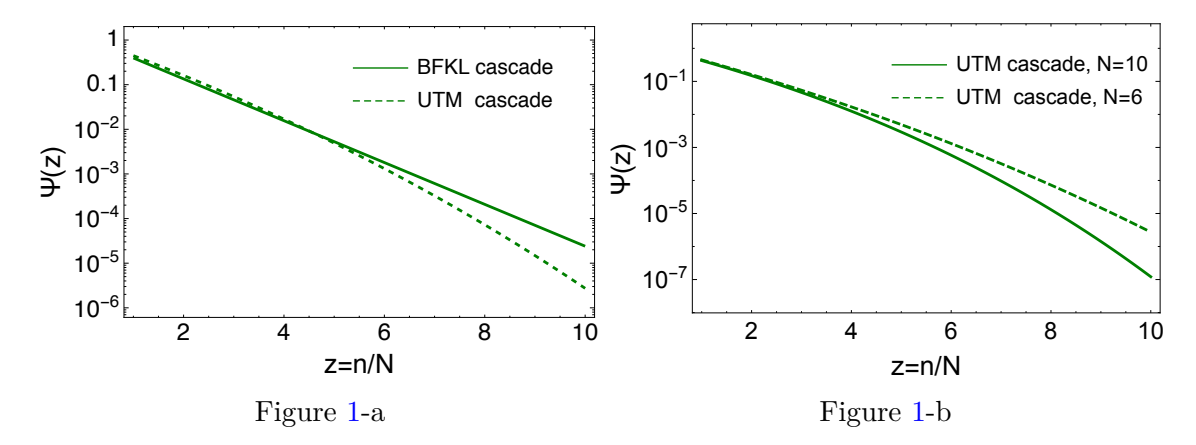


Figure 1-a: the KNO function  $\Psi\left(z=\frac{n}{N}\right)=NP_n$  for the BFKL cascade (eq. (2.32)) and the UTM cascade (eq. (2.52a)). Here N is the average multiplicity for the corresponding distribution, which is taken as N=6 in the figure. Figure 1-b shows that the KNO scaling for UTM is only approximate and the actual multiplicity distributions has more complex dependence on the mean multiplicity.

To find the function F that corresponds to a particular initial condition we need to match it to the solution of BK equation at small  $n\gamma$  calculated with the same initial condition. For the evolved single dipole matching with the solution of eq. (2.34) we obtain

$$P_{n(1)}^{\text{UTM}}(Y) = \frac{\gamma}{\left(1 - e^{-(n-1)\gamma}\right)} \exp\left(-e^{\zeta(Y,n)} + \zeta(Y,n)\right)$$

$$\xrightarrow{n\gamma < 1} e^{-\Delta Y} e^{-ne^{-\Delta Y}}$$

$$(2.52a)$$

In figure 1 we compare  $P_n$  of the BFKL cascade (eq. (2.32)) and of the UTM cascade with saturation given by eq. (2.52a).

To determine the range of validity of this calculation we consider

$$\frac{\partial P_{n(1)}^{\text{\tiny UTM}}}{\partial n} \!=\! \left[\gamma \!-\! e^{-\Delta Y + (n-1)\gamma}\right] P_{n(1)}^{\text{\tiny UTM}}; \quad \frac{\partial^2 P_{n(1)}^{\text{\tiny UTM}}}{\partial n^2} \!=\! \left[-\gamma e^{-\Delta Y + (n-1)\gamma} \!+\! \left[\gamma \!-\! e^{-\Delta Y + (n-1)\gamma}\right]^2\right] P_{n(1)}^{\text{\tiny UTM}} \quad (2.53)$$

First, we note that at high enough rapidity,  $Y > \frac{1}{\Delta} \ln \frac{1}{\gamma}$  the probability distribution has a maximum at

$$n_{\text{max}} - 1 = \frac{\Delta}{\gamma} Y - \frac{1}{\gamma} \ln \frac{1}{\gamma}$$
 (2.54)

Second, we see that for any fixed n at large enough Y we have  $\frac{d^2P_n}{dn^2} \ll \frac{dP_n}{dn}$  and therefore our approximation is valid. Moreover in the vicinity of the maximum  $n \sim n_{\text{max}}$  the calculation is valid at any rapidity. As is clear from eq. (2.53), parametrically the range of validity of the present approximation is given by

$$n - 1 < \frac{\Delta}{\gamma}Y\tag{2.55}$$

One can write down an approximate expression for the average multiplicity in the distribution  $P_{n(1)}^{\text{UTM}}$ . Approximating the sum over n by the integral while calculating N(Y) we

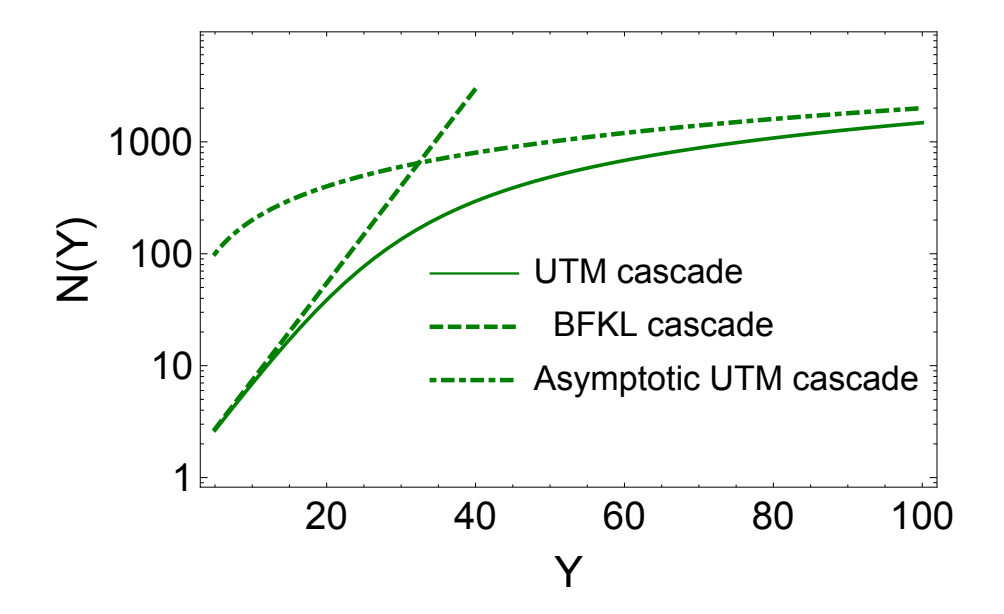


Figure 2. The mean multiplicity N(Y) (see eq. (2.56)) versus Y (solid curve). The mean multiplicity of the BFKL cascade is equal to  $\exp{(\Delta Y)}$ , the asymptotic multiplicity for the UTM cascade (see eq. (2.40)) is taken as  $N^{\rm asymp}(Y) = \frac{\Delta}{\gamma} Y$ .  $\Delta = 0.2$  and  $\gamma = 0.01$ .

find

$$N(Y) \equiv M_1(Y) \approx \frac{1}{\gamma} e^{\frac{1}{\gamma}e^{-\Delta Y}} \Gamma\left(0, \frac{1}{\gamma}e^{-\Delta Y}\right)$$
 (2.56)

where  $\Gamma(x,z)$  is an (upper) incomplete  $\Gamma$ -function [79].

From eq. (2.56) one can see that N(Y) reduces to the BFKL cascade value  $N(Y) \to \exp(\Delta Y)$  for small Y. On the other hand for large Y such that  $e^{-\Delta Y} \ll \gamma$  eq. (2.56) yields  $N(Y) \to \frac{\Delta}{\gamma} Y - \frac{1}{\gamma} \ln \frac{1}{\gamma}$  consistent with the value of  $n_{\text{max}}$  found in eq. (2.54). Interestingly this result for the average multiplicity is also consistent with the asymptotic limit of eq. (2.40), even though for very large Y our formal discussion above indicates that the range of validity of the approximation eq. (2.43) is limited by eq. (2.55).

In figure 2 we plot the dependence of the mean multiplicity N on rapidity for a single dipole initial condition, which demonstrates the above features. In figure 3 we plot the "history" of the distribution corresponding to the single dipole initial condition, starting with the BK evolution through the intermediate regime and into asymptotic rapidities.

#### 3 Generalizing UTM

The UTM satisfies the physical requirements of s- and t-channel unitarity, and also provides for saturation of emission probability at very high energies. Nevertheless it is quite clear that it is incomplete as far as the description of scattering of dense objects is concerned. The main culprit here is the fact, that only a single dipole is emitted in this model in one step of the evolution. This is obvious from the Mueller-Salam derivation as well as from the evolution equation for the RFT states (eq. (2.12)).

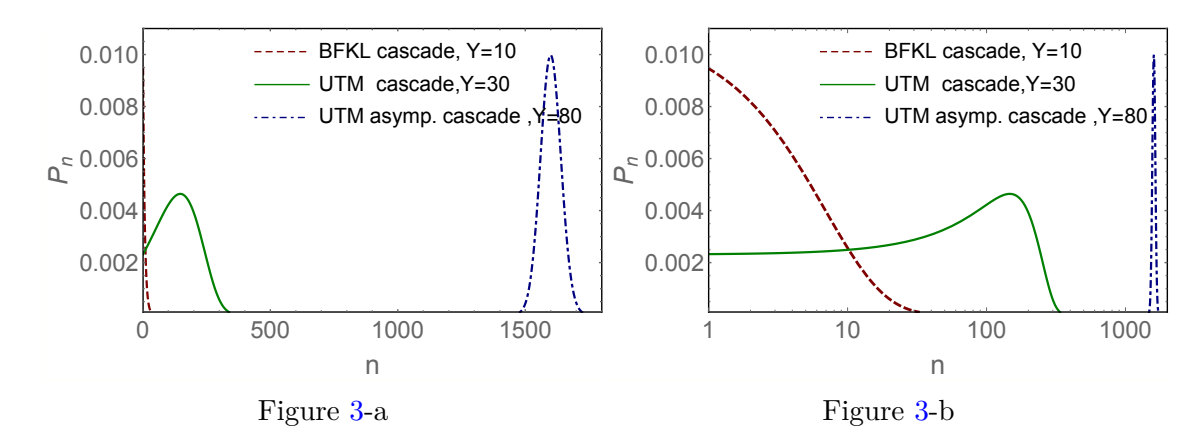


**Figure 3.**  $P_n(Y)$  versus n at different Y with the single dipole initial condition.  $\Delta = 0.2, \gamma = 0.01$ 

When the system is dense there is no reason why the number of dipoles emitted in one step of the evolution should be limited to one. Recall that the probability per unit rapidity for emission of a single dipole is of order  $\Delta n$  as long as  $n \leq 1/\gamma$ . Thus if the number of dipoles is large enough, i.e.  $n \geq 1/\Delta$  we expect that there is a sizable probability to emit extra dipoles, since the dipole emissions are in the first approximation independent in this range of n. Note that parametrically  $\Delta \sim \alpha_s$  while  $\gamma \sim \alpha_s^2$  thus we expect multiple dipole emissions to become important parametrically earlier than the saturation corrections. For n in the saturation regime, i.e.  $n \geq 1/\gamma$  the probability density (per unit rapidity) of emission of a single dipole is actually very large  $\sim 1/\alpha_s$  and multiple emissions in the wave function should be ubiquitous.

We note that in QCD at higher orders in perturbation theory the BFKL evolution indeed allows emission of more than one gluon, e.g. at NLO two gluons can be emitted. We will now discuss how multiple dipole emissions can be included in the toy model.

# 3.1 Emission of two gluons per one step of evolution

Our goal now is to include multiple dipole emissions without violating the s- and t-channel unitarity properties of the toy model. The Hamiltonian RFT formalism turns out to be a very convenient tool for this purpose. First, we already know that the t-channel unitarity is equivalent to the symmetry of the Hamiltonian under the transformation  $H(P, \bar{P}) \to H^T(\bar{P}, P)$ . The t-channel unitarity is therefore very easy to implement. The s-channel unitarity is slightly less transparent, but with a little trial and error we can find many s-channel unitary evolutions. This becomes particularly simple if we consider adding to  $H_{UTM}$  operators which are only (normal ordered) powers of  $\bar{P}P$ .

Consider the following simple perturbation on the Hamiltonian

$$\delta H_{\lambda} = \lambda \left(\frac{\Delta}{\gamma}\right)^2 : (\bar{P}P)^2 := \lambda \left(\frac{\Delta}{\gamma}\right)^2 \bar{P}^2 P^2$$
 (3.1)

where  $\lambda$  is a number of order unity. The counting of the powers of  $\alpha_s$  here is such that for small n we recover the NLO BFKL order of magnitude of the two gluon emission. The column here denotes the normal ordered operator, meaning that all factors of P have to be

placed to the right of the factors of  $\bar{P}$ . The *t*-channel unitarity is clearly preserved by  $\delta H_{\lambda}$ . With this additional term in the Hamiltonian, the evolution equation for  $P_n$  takes the form:

$$\frac{\partial P_n^{\lambda}(Y)}{\partial Y} = \frac{\Delta}{\gamma} \left[ -\left( (1 - e^{-\gamma n}) - \lambda \frac{\Delta}{\gamma} (1 - e^{-\gamma n})^2 \right) P_n^{\lambda}(Y) \right]$$
(3.2)

$$+\left(\left(1-e^{-\gamma(n-1)}\right)-\lambda\frac{\Delta}{\gamma}\left(1-e^{-\gamma(n-1)}\right)^2\right)P_{n-1}^{\lambda}(Y) \\ +\left.\lambda\frac{\Delta}{\gamma}\left(1-e^{-\gamma(n-2)}\right)^2P_{n-2}^{\lambda}(Y)\right]^2 \\ +\left(\left(1-e^{-\gamma(n-1)}\right)^2P_{n-2}^{\lambda}(Y)\right)^2P_{n-2}^{\lambda}(Y) + \left(1-e^{-\gamma(n-2)}\right)^2P_{n-2}^{\lambda}(Y) + \left(1-e^{-\gamma(n-2)}\right)^2P_{n-2}^{\lambda}(Y)$$

For  $\lambda \sim O(1) > 0$  the probabilities of emission of one and two dipoles are obviously positive, and the total probability is conserved, thus this evolution is s-channel unitary.

The RFT Schroedinger equation for the generating function now becomes

$$\frac{\partial Z_Y^\lambda(u)}{\partial Y} = \frac{\Delta}{\gamma} \left[ (u-1) \left( Z^\lambda - e^{-\gamma u \frac{\partial}{\partial u}} Z^\lambda \right) + \lambda \frac{\Delta}{\gamma} (1-u)^2 \left( Z^\lambda - 2e^{-\gamma u \frac{\partial}{\partial u}} Z^\lambda + e^{-2\gamma u \frac{\partial}{\partial u}} Z^\lambda \right) \right] \tag{3.3}$$

Just like for UTM, we can study the high energy asymptotics of the solution. Formally for  $\gamma u \frac{\partial}{\partial u} \gg 1$  we obtain the equation for the asymptotic generating function as:

$$\frac{\partial Z_Y^{\lambda \, asymp}(u)}{\partial Y} = \frac{\Delta}{\gamma} \left( (u - 1) + \lambda \frac{\Delta}{\gamma} (1 - u)^2 \right) Z_Y^{\lambda \, asymp}(u) \tag{3.4}$$

with the solution (here, as in the previous section we take the large Y limit and approximate the initial wave function at  $Y_0$  by a constant):

$$Z_Y^{\lambda \, asymp}(u) = \exp\left(\frac{\Delta}{\gamma} \left( (u-1) + \lambda \frac{\Delta}{\gamma} (1-u)^2 \right) Y \right)$$
 (3.5)

From this equation we can derive  $P_n^{\lambda}$ ,

$$P_n^{\lambda} = \oint \frac{e^{\frac{\Delta}{\gamma} \left( (u-1) + \lambda \frac{\Delta}{\gamma} (1-u)^2 \right) Y}}{u^{n+1}} du = \frac{1}{n!} \left[ \frac{d^n}{d u^n} e^{\frac{\Delta}{\gamma} \left( (u-1) + \lambda \frac{\Delta}{\gamma} (1-u)^2 \right) Y} \right]$$
(3.6)

The contour of integration in eq. (3.6) is the circle around u = 0. Now  $P_n$  does not follow the Poisson distribution anymore. Instead the distribution of dipoles has two independent factorial moments:  $M_1 = \langle n \rangle$  and  $M_2 = \langle n(n-1) \rangle$ :

$$M_1^{\lambda} = \frac{\partial}{\partial u} Z^{\lambda}(u)|_{u=1} = \frac{\Delta}{\gamma} Y; \quad M_2^{\lambda} = \frac{\partial^2}{\partial u^2} Z^{\lambda}(u)|_{u=1} = \left(\frac{\Delta}{\gamma}\right)^2 [Y^2 + 2\lambda Y]$$
 (3.7)

Clearly the additional term in the Hamiltonian modifies the asymptotic particle distribution. At first sight it may seem that at asymptotically large rapidities these corrections are small. Recall that the asymptotic solution is expected to be valid at such rapidities at which  $\langle n \rangle \gg 1/\gamma$ , which gives  $Y \gg 1/\Delta$ . At these rapidities, although the magnitude of

the correction to the second moment is large:  $\delta M_2 \sim \Delta/\gamma^2 \sim 1/\alpha^3$ , the relative correction is small  $\delta M_2/M_2 \sim \alpha_s$ . However factorial moments are not a very convenient measure of the shape of the distribution. If we want to get a better idea about the width of the distribution, for example we should not compare the second factorial moments but rather the variances  $\sigma^2 = \langle n^2 \rangle - \langle n \rangle^2$ . Here we find

$$\sigma_{UTM}^2 \xrightarrow{Y \to \infty} \frac{\Delta}{\gamma} Y; \qquad \sigma_{\lambda}^2 \xrightarrow{Y \to \infty} \left[ 2\lambda \frac{\Delta^2}{\gamma^2} + \frac{\Delta}{\gamma} \right] Y;$$
 (3.8)

It is now obvious that for non-vanishing positive  $\lambda$ , allowing emission of the second gluon renders the asymptotic distribution much wider  $\sigma_{\lambda}^2/\sigma_{UTM}^2 \sim 1/\alpha_s$ . Negative values of  $\lambda$  are not physical since they lead to negative probabilities and thereby s-channel unitarity violation, as is obvious from (3.2).

# 3.2 Emission of infinite number of gluons in one step of evolution

At high density it is not realistic to think that in one step of evolution a system of partons emits only one or two dipoles. Rather one expects that any number of gluons can be emitted with probabilities that scale as  $p_n \sim \Delta^n$  (modulo the saturation corrections). The exact values of these probabilities of course have to be determined by the underlying quantum field theory. Unfortunately in the toy world we do not have an underlying QFT, and the appropriate toy RFT cannot be strictly derived. Nevertheless one can make a simple reasonable assumption that leads to a definite form of RFT. Let us assume that the dipoles in one step of evolution are emitted independently of each other. This is certainly what one expects if the dipole density in the wave function is large enough but the saturation corrections are still unimportant. In the language of RFT Hamiltonian a single dipole emission is represented by the operator  $-\frac{\Delta}{\gamma}P\bar{P}$ . Given that the dipoles are indistinguishable bosons, the independent emission of n dipoles is represented by the operator  $\frac{1}{n!}(-\frac{\Delta}{\gamma}P\bar{P})^n$ . Since any number of emissions  $n \geq 1$  is allowed, we are lead to consider the RFT Hamiltonian

$$H_{UTMM} = : \left( e^{-\frac{\Delta}{\gamma}P\bar{P}} - 1 \right) : \tag{3.9}$$

where the additional M in the subscript stands for "Multiple Emissions". This Hamiltonian is also normal ordered so that all operators P appear to the right of all the operators  $\bar{P}$  in every order in the Taylor expansion of the exponential.  $H_{UTMM}$  reproduces UTM in the limit when  $\frac{\Delta}{\gamma}\bar{P}P$  is small, and contains eq. (3.1) with  $\lambda = 1/2$  as the first correction to UTM. It is obviously t-channel unitary.

When acting on an m-dipole state it yields:

$$H_{UTMM}|m\rangle = \left[e^{-\frac{\Delta}{\gamma}(1-e^{-\gamma m})(1-d)} - 1\right]|m\rangle$$

$$= \left[e^{-\frac{\Delta}{\gamma}(1-e^{-\gamma m})} - 1\right]|m\rangle + e^{-\frac{\Delta}{\gamma}(1-e^{-\gamma m})} \sum_{k=1}^{\infty} \frac{1}{k!} \left[\frac{\Delta}{\gamma}(1-e^{-\gamma m})\right]^{k} |m+k\rangle$$
(3.10)

This evolution of an m dipole state is clearly s-channel unitary as well.

Eq. (3.10) is equivalent to the equations for probabilities

$$\frac{dP_n^{\text{UTMM}}}{dY} = \left[ e^{-\frac{\Delta}{\gamma}(1 - e^{-\gamma n})} - 1 \right] P_n^{\text{UTMM}} + \sum_{k=1}^{\infty} \frac{1}{k!} e^{-\frac{\Delta}{\gamma}(1 - e^{-\gamma(n-k)})} \left[ \frac{\Delta}{\gamma} (1 - e^{-\gamma(n-k)}) \right]^k P_{n-k}^{\text{UTMM}}$$
(3.11)

The Schroedinger equation for this model is

$$\frac{dZ_Y^{\text{UTMM}}(u)}{dY} =: \left[ e^{-\frac{\Delta}{\gamma}(1-u)(1-e^{-\gamma u}\frac{\partial}{\partial u})} - 1 \right] : Z_Y^{\text{UTMM}}(u)$$
 (3.12)

where the normal ordering now refers to ordering of factors (1-u) and  $u\frac{\partial}{\partial u}$ .

The evolution eq. (3.10) has three distinct regimes. If the initial state contains a small number of dipoles,  $m \ll 1/\Delta$ , multiple emissions initially are unimportant and the cascade reduces to the BFKL-BK cascade. At higher rapidities where the typical dipole numbers are large but not "extremely large",  $1/\Delta < m < 1/\gamma$  one can still neglect the saturation corrections, as  $1 - e^{-\gamma n} \approx \gamma n$ , but multiple emissions have to be taken into account. And finally for asymptotically large rapidities where the properties of the wave function are dominated by very large dipole number configurations  $n > 1/\gamma$  one has to include both multiple emissions and the saturation corrections. If one starts the evolution with a single dipole state, these regimes will successively appear as the rapidity is increased. On the other hand if initially the number of dipoles is already very large (the "large nucleus" case), the system enters the saturated regime right away. We will discuss this situation in the next section. In this section we study the probability distribution which arises in the multiple emission regime without and with saturation corrections.

# 3.2.1 Multiple emissions without saturation $(\frac{1}{\Delta} < n < \frac{1}{\gamma})$

Let us first consider the regime where the rapidity is large enough so that multiple emissions are important, but is still too small for the saturation corrections to kick in. In terms of the dipole number n this is the regime where the bulk properties of the wave function are determined by  $\frac{1}{\Delta} < n < \frac{1}{\gamma}$ . The corresponding rapidity range will be given at the end of this section. In this regime we expect UTMM to differ significantly from UTM. On the other hand at these rapidities the properties of the UTM distribution are the same as those of BFKL cascade, as discussed in the previous section. In this section we will thus compare the properties of UTMM cascade with those of BFKL, which equivalently can be thought of as a comparison between the UTMM and UTM cascades.

For small  $\gamma n$  using  $1 - e^{-\gamma n} \approx n\gamma$  the evolution equation for probabilities becomes

$$\frac{dP_n^{\text{UTMM}}}{dY} = \left[ e^{-\Delta n} - 1 \right] P_n^{\text{UTMM}} + \sum_{k=1}^{\infty} \frac{1}{k!} e^{-\Delta(n-k)} \left[ \Delta(n-k) \right]^k P_{n-k}^{\text{UTMM}} 
= -P_n^{\text{UTMM}} + \sum_{k=0}^{\infty} \frac{1}{k!} e^{-\Delta(n-k)} \left[ \Delta(n-k) \right]^k P_{n-k}^{\text{UTMM}}$$
(3.13)

We note that this equation is consistent with normalization of probability, as summing eq. (3.13) over n we find that  $\frac{d}{dY} \sum_n P_n^{\text{UTMM}} = 0$ .

The Schroedinger equation in this limit becomes

$$\frac{dZ_Y^{\text{UTMM}}(u)}{dY} =: \left[ e^{-\Delta(1-u)u\frac{\partial}{\partial u}} - 1 \right] : Z_Y^{\text{UTMM}}(u) \tag{3.14}$$

Just like in the BK limit, the no-saturation limit of UTMM is not sensitive to the value of  $\gamma$ —the only constant that enters here is the emission probability  $\Delta$ . To study the properties of the resulting probability distribution, we rewrite eq. (3.13) as evolution equation for the factorial moments. Let us start with the mean multiplicity  $M_1^{\rm UTMM}$ . Eq. (3.13) takes the form

$$\frac{dM_1^{\text{UTMM}}}{dY} = -M_1^{\text{UTMM}} + \sum_{k=0,n=1}^{\infty} \left(n - k + k\right) \frac{1}{k!} e^{-\Delta(n-k)} \left[\Delta(n-k)\right]^k P_{n-k}^{\text{UTMM}} 
= -M_1^{\text{UTMM}} + \Delta M_1^{\text{UTMM}} + M_1^{\text{UTMM}} = \Delta M_1^{\text{UTMM}}$$
(3.15)

We consider the initial conditions corresponding to a single dipole initial state  $M_k^{\text{UTMM}}(Y = 0) = \delta_{k1}$ . With this initial condition the solution is

$$M_1^{\text{UTMM}}(Y) = e^{\Delta Y} \tag{3.16}$$

Interestingly the mean multiplicity turns out to be the same as for BK distribution (see eq. (2.32)). For  $M_2^{\text{UTMM}}$  we have

$$\frac{dM_{2}^{\text{UTMM}}}{dY} = -M_{2}^{\text{UTMM}} + \sum_{k=0,l=1}^{\infty} \left( (k+l)^{2} - (k+l) \right) \frac{1}{k!} e^{-\Delta(l)} \left[ \Delta(l) \right]^{k} P_{l}^{\text{UTMM}} 
= -M_{2}^{\text{UTMM}} + M_{2}^{\text{UTMM}} + \left( 2\Delta + \Delta^{2} \right) \left( M_{2}^{\text{UTMM}} + M_{1}^{\text{UTMM}} \right) 
= \left( 2\Delta + \Delta^{2} \right) \left( M_{2}^{\text{UTMM}} + M_{1}^{\text{UTMM}} \right)$$
(3.17)

For a single dipole initial condition the solution for  $M_2^{\text{UTMM}}$ :

$$M_2^{\text{UTMM}}(Y) = \frac{(2+\Delta)}{(\Delta+1)} \left( e^{(2+\Delta)\Delta Y} - e^{\Delta Y} \right)$$
(3.18)

For  $M_3^{\text{UTMM}}$  the equation is:

$$\begin{split} \frac{dM_{3}^{\text{UTMM}}}{dY} &= -M_{2}^{\text{UTMM}} + \sum_{k=0,l=1}^{\infty} \left( (k+l)^{3} - 3(k+l)^{2} + 2(k+l) \right) \frac{1}{k!} e^{-\Delta(l)} \left[ \Delta(l) \right]^{k} P_{l}^{\text{UTMM}} \\ &= -M_{3}^{\text{UTMM}} + M_{3}^{\text{UTMM}} + \left( (1+\Delta)^{3} - 1 \right) \left( M_{3}^{\text{UTMM}} + 3M_{2}^{\text{UTMM}} + M_{1}^{\text{UTMM}} \right) \\ &- 3\Delta \left( M_{2}^{\text{UTMM}} + M_{1}^{\text{UTMM}} \right) \\ &= \left( (1+\Delta)^{3} - 1 \right) M_{3}^{\text{UTMM}} + 3\Delta (1+\Delta) \left( 2 + \Delta \right) M_{2}^{\text{UTMM}} + \Delta^{2} \left( 3 + \Delta \right) M_{1}^{\text{UTMM}} \end{split}$$

with the solution

$$M_3^{\rm UTMM} = \frac{e^{\Delta Y} \left( (\Delta + 1)(\Delta(2\Delta + 9) + 12) - 3(\Delta + 2)^3 e^{\Delta(\Delta + 1)Y} + (\Delta + 4)(\Delta(\Delta + 3) + 3)e^{\Delta(\Delta + 1)(\Delta + 2)Y} \right)}{(\Delta + 1)^2 (\Delta + 2)} \tag{3.20}$$

Considering  $\Delta \ll 1$  we can simplify eq. (3.18) and eq. (3.20) (we do not neglect corrections due to nonvanishing  $\Delta$  in the exponent, but only in the prefactors):

$$M_2^{\text{UTMM}}(Y) = 2! \left( e^{((1+\Delta)^2 - 1)Y} - e^{\Delta Y} \right);$$

$$M_3^{\text{UTMM}}(Y) = 3! \left( e^{((1+\Delta)^3 - 1)Y} - 2e^{((1+\Delta)^2 - 1)Y} + e^{\Delta Y} \right)$$
(3.21)

For  $\Delta^2 Y \ll 1$  we see that  $M_2^{\rm UTMM} \approx 2 M_1^{\rm UTMM} \left( (M_1^{\rm UTMM})^{1+\Delta} - 1 \right)$  and the second moment of UTMM is very close to that of the BK multiplicity distributions of eq. (2.32). The same holds for the third moment (neglecting  $\Delta$  in the exponent)  $M_3^{\rm UTMM} \approx 3! \, M_1^{\rm UTMM} \, (M_1^{\rm UTMM} - 1)^2$ . At much larger rapidities  $\Delta^2 Y > 1$  the difference between the moments in UTMM and BK is significant, and the above expressions for both  $M_2^{\rm UTMM}$  and  $M_3^{\rm UTMM}$  are much larger than in the BK limit. However we should keep in mind that the above expressions for  $M_k^{\rm UTMM}$  are representative of the UTMM only for  $M_1^{\rm UTMM} < 1/\gamma$ , which translates into  $Y < \frac{1}{\Delta} \ln \frac{1}{\gamma}$ . For rapidities  $Y \gg 1/\Delta^2 \sim 1/\gamma$  the saturation corrections take over and the actual distribution is not described faithfully by the solution to eq. (3.13). Thus rapidities  $Y \sim \frac{1}{\Delta^2}$  are strictly speaking outside the range of validity of our present approximation.

Thus for rapidities that we may consider, the expressions in eqs. (3.18), (3.21) are (up to perturbative corrections) the same as in the BFKL -BK regime. This at the first glance looks strange, since the UTM allows emissions of multiple dipoles in one step of the evolution. The reason we do not get on average more dipoles in the wave function, as well as nearly identical second and third moments of the distribution, is because the exponential form of the Hamiltonian includes a kind of "unitarization corrections", i.e. since many dipoles are allowed to be emitted, the probability of emission of a single dipole is smaller than in the BK model (at the same value of parameter  $\Delta$ ). Nevertheless even in the allowed region we expect the distribution to differ significantly from BK. Indeed, examining higher moments we see that this is the case. Let us consider only the leading term in the k-th moment, i.e. the term with the fastest growth in rapidity. For this term it is easy to write the general expression ( see appendix A)

$$M_k^{\text{UTMM}}(Y) \propto e^{((1+\Delta)^k - 1)Y} \tag{3.22}$$

Consider high moments, so that  $k = \frac{K}{\Delta}$ . For very small  $\Delta$  we have  $(1 + \Delta)^{\frac{1}{\Delta}} \approx e$ , and thus

$$M_k^{UTMM}(Y) \propto e^{(e^K - 1)Y} \tag{3.23}$$

while for the same k the leading behavior in the BK model is

$$M_k^{BK} \propto e^{KY} \tag{3.24}$$

Thus for large k the moments differ already in the leading order term with

$$M_k^{UTMM} \gg M_k^{BK} \tag{3.25}$$

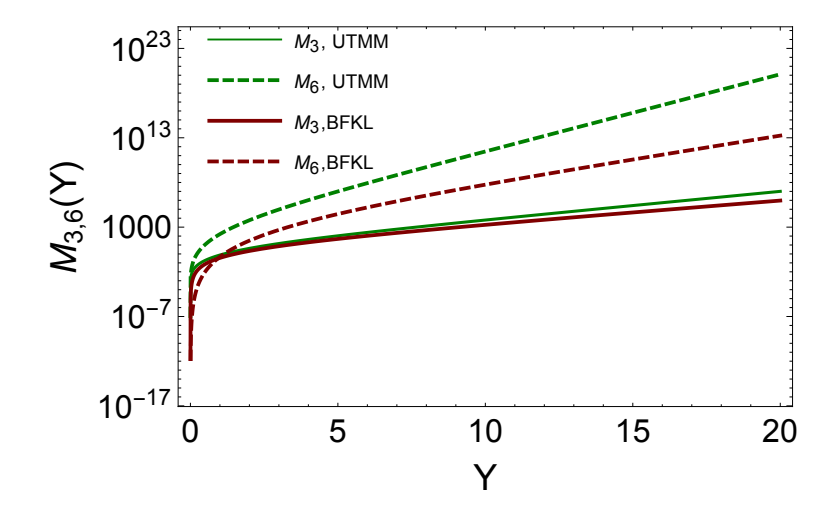


**Figure 4.**  $M_k$  versus Y. The green curves describe the exact solution to eq. (3.20) for the UTMM cascade and eq. (A.4), while the red ones correspond to the BFKL multiplicity distributions of eq. (2.33).  $\Delta = 0.2$ .

We conclude that, just like expected the probability distribution is significantly wider in the "multiple emission" regime of UTMM compared to BFKL-BK cascade. In figure 4 we plot the third and sixth moments for illustration and indeed see that while  $M_3$  in both cascades is very similar at intermediate rapidities,  $M_6$  is significantly larger in UTMM.

In principle, once the factorial moments are given, one can reconstruct the probability distribution. In the present case this turns out to be tricky since the moments grow very fast at large k and one is faced with a necessity to sum an asymptotic series. In appendix A we discuss a way to resolve this issue and give a derivation of the (approximate) probability distribution. The result is

$$P_n^{\text{UTMM}}(Y) = e^{-Y} \sum_{j=0}^{\infty} \frac{Y^j}{j!} P_n^j \quad \text{with} \quad P_n^j = \frac{1}{N_j} \left( 1 + \frac{1}{N_j} \right)^{-n}$$
 (3.26)

where  $N_j = (1 + \Delta)^j$ .

In figure 5 we show the values of  $P_n^{UTMM}$  from eq. (3.26) versus n at different values of Y. Figure 5-a shows that in the region of small n the UTMM multiplicity distribution is close to BFKL cascade but at large n the deviation is rather large. This is consistent with our discussion of high factorial moments. Figure 5-b shows that although UTMM cascade strictly speaking violates KNO scaling, these violations are not large in practice.

Finally we note that we can estimate the range of rapidities in which the evolution is dominated by multiple emissions, but saturation is still not important. The relevant condition in terms of the average mulitplicity is  $1/\Delta < M_1^{\text{UTMM}} < 1/\gamma$ , which given eq. (3.16) in terms of rapidity translates into  $\frac{1}{\Delta} \ln \frac{1}{\Delta} < Y < \frac{1}{\Delta} \ln \frac{1}{\gamma}$ .

# 3.2.2 The S-matrix for single and multiple gluon emissions

Although our main focus in this paper is in the probability distributions, it is interesting to see how allowing multiple emission affects more directly measurable physical quantities.

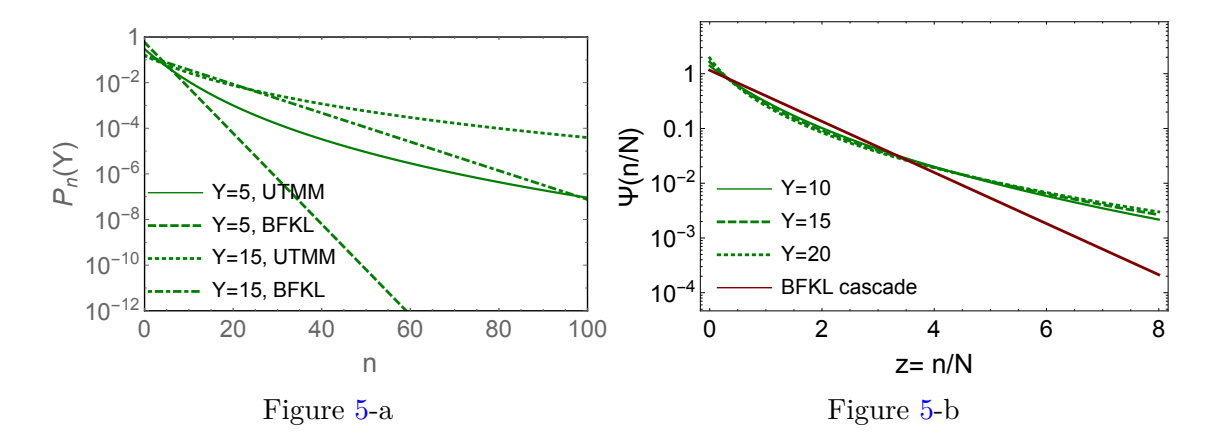


**Figure 5.** Figure 5-a:  $P_n(Y)$  versus n at fixed values of Y from eq. (3.26). Figure 5-b: the KNO function  $\Psi(z) = NP_{zN}$  where N is the mean multiplicity.  $\Delta = 0.2$ . BFKL cascade denotes the distribution of eq. (2.32).

The S-matrix can be calculated using (2.8) [23]. For UTM in the kinematic regime under consideration we can use the probabilities given in eq. (2.34)

$$S(Y) = \sum_{n,m=0}^{\infty} e^{-m \, n \, \gamma} \, P_n^{\text{BFKL}}(Y_0) \, P_m^{\text{BFKL}}(Y - Y_0)$$

$$= \int_0^{\infty} \frac{dn}{n} \, du \, e^{-\gamma \, u} \frac{1}{N(Y_0) \, N(Y - Y_0)} \, \exp\left(-\frac{n}{N(Y_0)} - \frac{u}{n \, N(Y - Y_0)}\right)$$

$$= -\frac{e^{\frac{1}{\gamma N(Y)}} \text{Ei}\left(-\frac{1}{N(Y)\gamma}\right)}{\gamma N(Y)}$$
(3.27)

where Ei(z) is the exponential integral:  $Ei(z) = -E_1(z) = \int_{-\infty}^{z} \frac{e^{\xi}}{\xi} d\xi$ .

For the total cross section we have<sup>3</sup>

$$\sigma_{\text{tot}} = 2A(Y) = 2(1 - S(Y))$$
 (3.28)

We can also estimate the inelastic cross section, using the approach of [23]

$$\sigma_{\rm in} = 1 - \sum_{n,m} e^{-2 m n \gamma} P_n(Y_0) P_m(Y - Y_0)$$
(3.29)

In general the inelastic cross section defined in eq. (3.29) is not independent of frame, i.e. depends on  $Y_0$  [23]. However for the probability distribution eq. (2.34) we find an  $Y_0$ -independent result

$$\sigma_{\rm in} = A(Y, \gamma \to 2\gamma) = 1 + \frac{e^{\frac{1}{2\gamma N(Y)}} \operatorname{Ei}\left(-\frac{1}{2\gamma N(Y)}\right)}{2\gamma N(Y)}$$
(3.30)

<sup>&</sup>lt;sup>3</sup>This is a slight abuse of language, as in the toy model there is no transverse dimension, and thus no cross section. The quantities we calculate in this subsection are dimensionless, and are simply proportional to the appropriate probabilities. We will nevertheless refer to them as cross sections using the higher dimensional analogy.

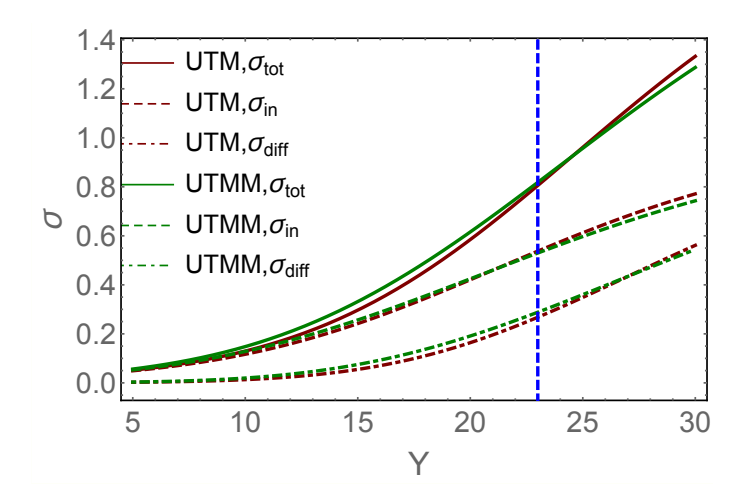


**Figure 6.** The inclusive observable in UTM and UTMM versus Y.  $\Delta = 0.2$  and  $\gamma = 0.01$ .

With  $\sigma_{\rm tot}$  and  $\sigma_{\rm in}$  we can estimate the cross section for diffraction production (  $\sigma_{diff}$ ):

$$\sigma_{diff} = \sigma_{\text{tot}} - \sigma_{\text{in}}$$
 (3.31)

With this definition  $\sigma_{diff}$  includes the elastic cross section. The cross section for diffractive dissociation is obtained by subtracting for  $\sigma_{diff}$  the elastic cross section

$$\sigma_{dd} = \sigma_{diff} - (A(Y))^2 \tag{3.32}$$

For UTMM, replacing  $P_n$  in eq. (3.27) by eq. (3.26) we obtain

$$S^{\text{UTMM}}(Y) = \sum_{n,m} e^{-m \, n \, \gamma} \, P_n^{\text{UTMM}}(Y_0) \, P_m^{\text{UTMM}}(Y - Y_0)$$

$$= e^{-Y} \sum_{j_1} \sum_{j_2} \frac{Y_0^{j_1} \, (Y - Y_0)^{j_2}}{j_1! \, j_2!} \int_0^\infty \frac{dn}{n} \, du \, e^{-\gamma \, u} \frac{1}{N_{j_1} N_{j_2}} \, \exp\left(-\frac{n}{N_{j_1}} - \frac{u}{n \, N_{j_2}}\right)$$

$$= -e^{-Y} \sum_{j} \frac{Y^{j}}{(j)!} \frac{e^{\frac{1}{\gamma N_j}} \operatorname{Ei}\left(-\frac{1}{\gamma N_j}\right)}{\gamma \, N_j}$$
(3.33)

Using eq. (3.33) in eqs. (3.28)–(3.32) we obtain the physical observables in the UTMM. In figure 6 and figure 7 we plot the various cross sections for the two models (UTM and UTMM). The kinematic region where saturation corrections are not important extends only up to rapidity  $Y_{\text{max}} = \frac{1}{\Delta} \ln \frac{1}{\gamma}$ . denoted by the vertical line on the graphs. We nevertheless plot the curves up to higher rapidities to illustrate an interesting point that indeed around  $Y_{\text{max}}$  the various quantities exhibit qualitative change of behavior. The differences between the two models follow the expected trend. The total cross section in UTMM is higher than in UTM, since it has larger probability to have higher number of dipoles. The cross section for diffractive dissociation on the other hand is lower in UTMM, consistent with the fact that it involves subtraction of the square of elastic amplitude, which is sensitive to the fluctuation in the dipole number. In fact one can see from the graphs that among the quantities we calculated,  $\sigma_{dd}$  is the best discriminator between UTM and UTMM.

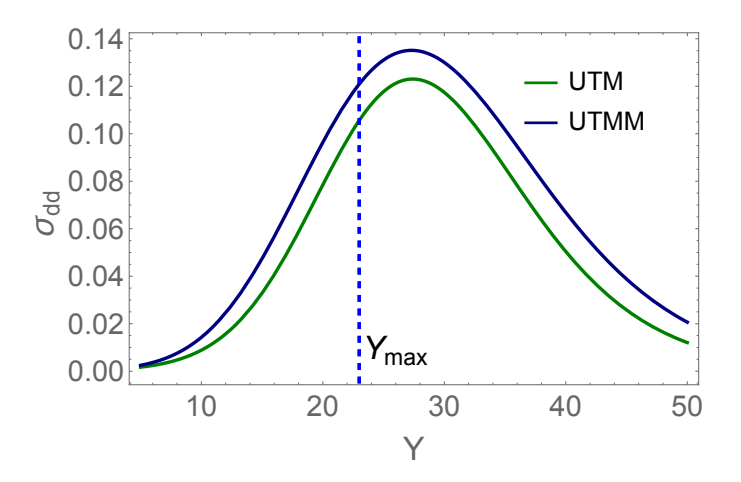


Figure 7. The cross section of diffraction dissociation  $\sigma_{dd} = \sigma_{diff} - \sigma_{el}$  from eq. (3.31), for UTM and UTMM versus Y.  $\Delta = 0.2$  and  $\gamma = 0.01$ .

# 3.2.3 Multiple emissions with saturation — large Y asymptotics $(n\gg \frac{1}{\gamma})$

For very large n the term  $\exp(-\gamma n) \ll 1$  can be neglected and equations for  $P_n$  take the form:

$$\frac{d P_n^{\text{UTMM}}(Y)}{dY} = \left(e^{-\frac{\Delta}{\gamma}} - 1\right) P_n^{\text{UTMM}}(Y) + e^{-\frac{\Delta}{\gamma}} \sum_{k=1}^{\infty} \frac{1}{k!} \left(\frac{\Delta}{\gamma}\right)^k P_{n-k}^{\text{UTMM}}(Y)$$
(3.34)

and the asymptotic form of the RFT Schroedinger equation is:

$$\frac{d Z_{\text{asymp}}^{\text{UTMM}}(Y)}{d y} = \left(e^{\frac{\Delta}{\gamma}(u-1)} - 1\right) Z_{\text{asymp}}^{\text{UTMM}}(Y)$$
(3.35)

This has an obvious solution:

$$Z_{\text{asymp}}^{\text{UTMM}} = \exp\left(\left(e^{\frac{\Delta}{\gamma}(u-1)} - 1\right)Y\right)$$
 (3.36)

where, as before we have neglected a possible slow varying prefactor  $Z_{Y_0}(u)$  arising from initial condition. These equations describe the asymptotics of the distribution in UTMM at very large Y.

The factorial moments are obtained using eq. (3.6) and the asymptotic solution of eq. (3.36). For the first three factorial moments we then obtain

$$M_1^{\text{UTMM}} = \frac{\Delta}{\gamma} Y; \quad M_2^{\text{UTMM}} = \frac{\Delta^2}{\gamma^2} Y^2 + \frac{\Delta^2}{\gamma^2} Y; \quad M_3^{\text{UTMM}} = \frac{\Delta^3}{\gamma^3} Y^3 + 3\frac{\Delta^3}{\gamma^3} Y^2 + \frac{\Delta^3}{\gamma^3} Y \quad (3.37)$$

One can write the moments in the following explicit form

$$M_k^{\text{UTMM}} = \left(\frac{\Delta}{\gamma} t \frac{d}{dt}\right)^k e^{(t-1)Y}|_{t=1}$$
 (3.38)

with

$$t \equiv \exp\left(\frac{\Delta}{\gamma}(u-1)\right) \tag{3.39}$$

Similar representation for the probabilities is

$$P_n^{\text{UTMM}}(Y) = \frac{1}{n!} \left( \frac{\Delta}{\gamma} t \frac{d}{dt} \right)^n e^{(t-1)Y} \Big|_{t=e^{-\frac{\Delta}{\gamma}}}$$
(3.40)

Another representation can be obtained expanding the exponent  $e^{tY}$ :

$$P_n^{\text{UTMM}}(Y) = \frac{1}{n!} \left( \frac{\Delta}{\gamma} t \frac{d}{dt} \right)^n e^{(t-1)Y} \Big|_{t=e^{-\frac{\Delta}{\gamma}}} = \frac{1}{n!} e^{-Y} \left( \frac{\Delta}{\gamma} t \frac{d}{dt} \right)^n \sum_{k=0}^{\infty} \frac{(Yt)^k}{k!} \Big|_{t=e^{-\frac{\Delta}{\gamma}}}$$

$$= \frac{1}{n!} e^{-Y} \sum_{k=0}^{\infty} \frac{1}{k!} \left( \frac{\Delta}{\gamma} k \right)^n \left( Ye^{-\frac{\Delta}{\gamma}} \right)^k$$
(3.41)

An interesting question is what is the range of k that contributes to the sum in eq. (3.41). For large rapidity we expect that the most important values of n are large, and k for these n is also large. For large k we can estimate the range by replacing the sum with the integral over k and finding the maximum of the integrand. The equation for the saddle point,  $k_{SP}$  has the form:

$$\frac{d\Psi}{dk}|_{k=k_{SP}} = 0 \quad \text{with } \Psi = n\left(\ln\left(\frac{\Delta}{\gamma}\right) + \ln\left(k\right)\right) - k\left(\ln\left(\frac{k}{\mathcal{Y}}\right) - 1\right); \qquad \frac{n}{k_{SP}} - \ln\frac{k_{SP}}{\mathcal{Y}} = 0; \tag{3.42}$$

where  $\mathcal{Y} = Y \exp\left(-\frac{\Delta}{\gamma}\right)$ . The approximate solution for  $k_{SP}$  is

$$k_{SP} = \frac{n}{\ln\left(\frac{n}{\mathcal{Y}}\right)} \tag{3.43}$$

Note that  $e^{-\frac{\Delta}{\gamma}}$  is an exponentially small number, thus for reasonable values of Y we have  $\mathcal{Y} \ll 1$ . Hence  $k_{SP} \ll n$  and the ratio between the two decreases for large n.

It is tempting to estimate the sum in eq. (3.41) by the method of steepest descent, however it turns out that the maximum in k is very broad and the steepest descent method is not applicable. Nevertheless eq. (3.42) gives a good estimate of the important range of k. Limiting summation over k in eq. (3.41) by  $k_{\text{max}}$ , we find that  $k_{\text{max}} = 2k_{SP}$  gives a very good agreement with the exact sum (see figure 8).

We plot the distribution given by eq. (3.41) in figure 8 and compare it to the Poisson distribution eq. (2.40) with the same mean value. This latter distribution as discussed previously, is the asymtotic distribution in UTM. Clearly the distribution of eq. (3.41) is much broader. On the other hand figure 8-c illustrates that eq. (3.41) is well approximated by the normal distribution (ND) with the mean value  $\langle n \rangle = \frac{\Delta}{\gamma} Y$  and variance  $\sigma^2 = \left(\frac{\Delta^2}{\gamma^2} + \frac{\Delta}{\gamma}\right) Y$  as suggested by eq. (3.37),

$$P_n^{ND} = \frac{1}{\sqrt{2\pi\sigma^2}} \exp\left(-\frac{(n-\langle n \rangle)^2}{2\sigma^2}\right)$$
 (3.44)

Figure 8-d demonstrates that an equally good approximation is provided by the negative binomial distribution

$$P_n^{NBD} = \frac{\left(\frac{r}{N+r}\right)^r \left(\frac{N}{N+r}\right)^n \Gamma(n+r)}{n!\Gamma(r)}$$
(3.45)

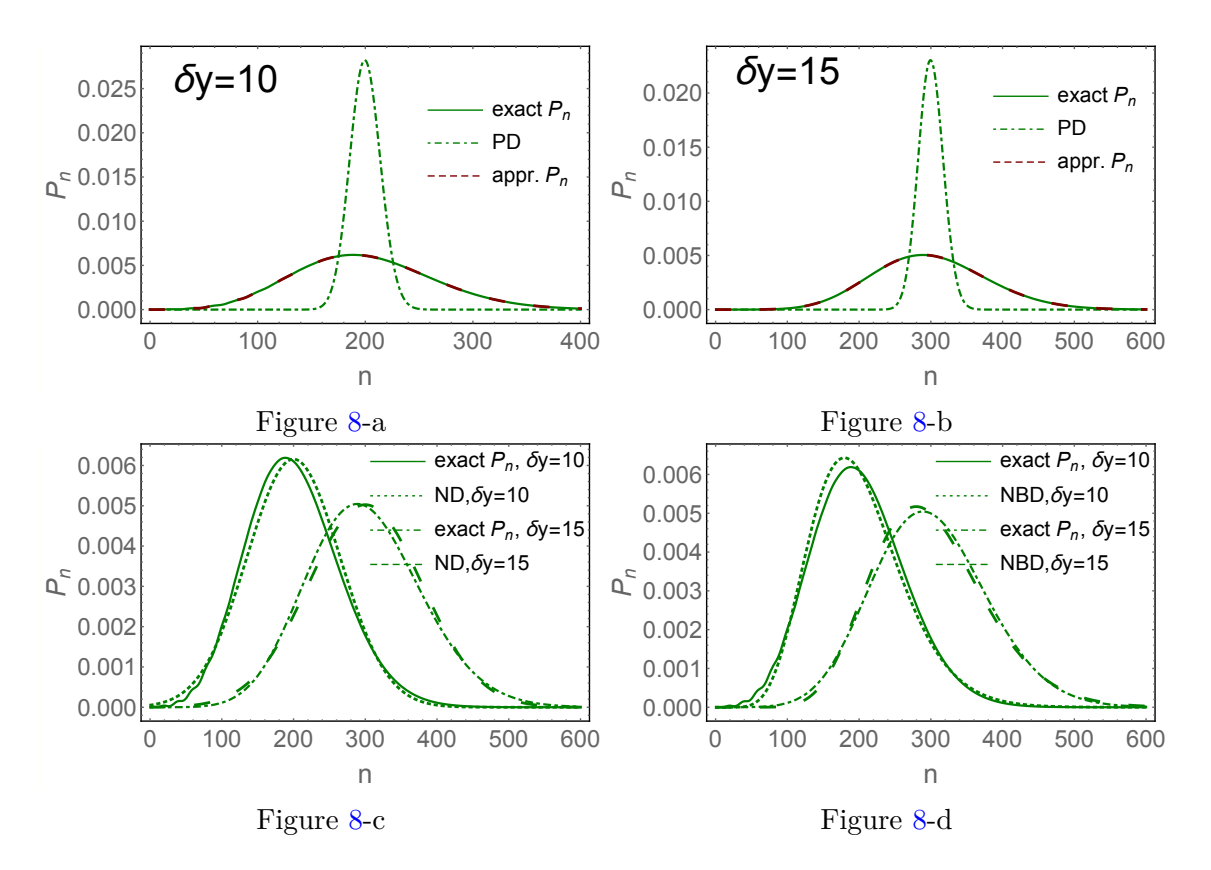


Figure 8. Multiplicity distributions for two values of Y. The exact  $P_n$  denote the distribution of eq. (3.41), the approximate  $P_n$  are the multiplicity distributions in which we sum over k from k = 0 up to  $k_{\text{max}} = 2k_{SP}$ . PD is the Poisson distribution of eq. (2.40). ND and NBD (see text) denote the normal and negative binomial distributions.  $\frac{\Delta}{\gamma}$  is taken to be equal to 20.  $\delta y$  denotes the amount of evolution from the initial rapidity  $Y_0$  to Y, see eq. (2.38).

with the mean value  $N=M_1^{\rm UTMM}$  and parameter  $r=\frac{M_1^2}{M_2-M_1^2}=Y$ . In fact  $P^{NBD}$  reproduces the first and the second terms in all  $M_k^{\rm UTMM}$  of eq. (3.37)., viz:  $M_k^{\rm UTMM}=N^k\left(1+\frac{k(k-1)}{2}\frac{1}{Y}+O\left(\frac{1}{Y^2}\right)\right)$ .

As expected therefore, allowing multiple dipole emissions results in a qualitatively different, and much broader distribution. This is true both at intermediate rapidities, where the saturation is unimportant, and also at asymptotically large energies where the saturation effects play crucial role. Interestingly, in both regimes the average number of dipoles at a given rapidity is the same in UTM and UTMM, and it is the shape of the distribution that discriminates decisively between the two models.

# 4 "Nuclei" and evolution: the m-dipole initial condition

In this paper our primary interest is in the regime where multiple emissions in the evolution are important. For an initial condition of a single dipole this regime is achieved only at large rapidities. It is interesting to consider how the situation changes if our initial condition itself contains multiple dipoles. Such an initial condition is a proxy to a "nucleus" in the toy world. We expect naturally, that in this case the asymptotic regime in the evolution

will be achieved at much lower rapidities. In this section we repeat the analysis of the evolution for the initial condition of exactly m dipoles at initial rapidity. In terms of the initial probability distribution this means

$$P_{n(m)}(Y=0) = \delta_{nm} \tag{4.1}$$

while in terms of factorial moments:

$$M_{k(m)}(Y=0) = \frac{m!}{(m-k)!}; \quad k \le m; \qquad M_{k(m)}(Y=0) = 0; \quad k > m$$
 (4.2)

or in terms of the wave function

$$Z_0(u) = u^m (4.3)$$

## 4.1 Many dipoles evolved with BK

For the BK evolution the solution for the m-dipole initial condition is easy to find. Using eq. (2.29) and eq. (4.3) we find

$$Z_Y^{BK}(u;m) = \left[\frac{u}{u(1 - e^{\Delta Y}) + e^{\Delta Y}}\right]^m. \tag{4.4}$$

With this generating function the probabilities are found to be

$$P_{n(m)}^{BK}(Y) = C_{m-1}^{m-1} e^{-m\Delta Y} \left[ 1 - e^{-\Delta Y} \right]^{n-m}. \tag{4.5}$$

The binomial coefficient  $C_{m-1}^{n-1}$  here is simply the number of ways to put n identical objects into m boxes without leaving a single box empty.

The first moment is also easily calculated

$$M_{1(m)}^{BK} \equiv N_{(m)}(Y) = me^{\Delta Y}$$
 (4.6)

while for the k-th moment we get

$$M_{k(m)}^{BK} = k! e^{k\Delta Y} \sum_{l=1}^{m} C_{l}^{m} C_{l-1}^{k-1} \left[ 1 - e^{-\Delta Y} \right]^{k-l} = k! e^{\Delta k Y} m T^{k-1} {}_{2}F_{1} \left( 1 - k, 1 - m; 2; \frac{1}{T} \right)$$

$$(4.7)$$

where  $T = 1 - \exp(-\Delta Y) = 1 - \frac{m}{N_{(m)}}$ . For large rapidities

$$P_{n(m)}^{BK}(Y) \xrightarrow{\Delta Y \gg 1} \frac{(n-1)!}{(n-m)!(m-1)!} \left(\frac{m}{N_{(m)}(Y)}\right)^m \exp\left[-\frac{m(n-m)}{N_{(m)}(Y)}\right]$$

$$\xrightarrow{n \gg m; \ e^{\Delta Y} \gg m} \frac{m}{(m-1)!} \frac{1}{N_{(m)}(Y)} \left(\frac{mn}{N_{(m)}(Y)}\right)^{m-1} \exp\left[-\frac{mn}{N_{(m)}(Y)}\right]$$
(4.8a)

$$M_{k(m)}^{BK} \xrightarrow{e^{\Delta Y} \gg m} \left(\frac{N_{(m)}(Y)}{m}\right)^k \frac{(m+k-1)!}{(m-1)!}$$
 (4.8b)

We note that for m=1 the probability distribution at high energy satisfies the KNO scaling. For m>1 this is strictly speaking not true, however at high enough energy where  $\exp\{\Delta Y\}\gg m$  and only large values of  $n\gg m$  matter for the bulk properties of the distribution the KNO scaling is restored as is clear from eq. (4.8a). Nevertheless even at high energies the initial number of dipoles m appears as a parameter in the KNO function. In particular the KNO function drops faster at large values of the argument for large m.

# 4.2 *m*-dipoles in UTM at intermediate rapidities

The initial condition determines matching of the solution of UTM with the BK regime. Matching eq. (2.50) with eq. (4.8a) at small Y we obtain

$$P_{n(m)}^{\text{UTM}}(Y) = \frac{1}{(m-1)!} \frac{\gamma}{(1 - e^{-(n-1)\gamma})} \exp\left(-e^{\zeta(Y,n)} + m\zeta(Y,n)\right)$$
$$= \frac{1}{(m-1)!} e^{-\Delta Y + \gamma(n-1)} \exp\left(-e^{\zeta(Y,n)} + (m-1)\zeta(Y,n)\right); \quad (4.9)$$

This qualitatively is rather similar to the solution for m = 1. In fact the sensitivity to the value of m is weaker in this regime than for the BFKL cascade.

The value of n at which the probability eq. (4.9) is maximal is determined with good accuracy from the relation

$$\zeta(Y,n) = \ln(m) \tag{4.10}$$

or from vanishing of the derivative

$$\frac{\partial P_{n(m)}^{\text{UTM}}}{\partial n} = \left[ \gamma \left[ 1 + \frac{m-1}{1 - e^{-(n-1)\gamma}} \right] - e^{-\Delta Y + (n-1)\gamma} \right] P_{n(m)}^{\text{UTM}}; \tag{4.11}$$

Taking m as a number which is parametrically not large  $m \ll 1/\gamma$ , we find that at large rapidity the maximum of the probability distribution is at

$$n_{\text{max}}^{(m)} - 1 \approx \frac{\Delta}{\gamma} Y - \frac{1}{\gamma} \ln \frac{1}{m\gamma}$$
 (4.12)

This relation clearly exhibits effects of saturation: the value of  $n_{\text{max}}^{(m)}$  grows only logarithmically with m, whereas if we were to continue the BFKL cascade to these values of rapidity, the position of the maximum would be linear in m.

For the mean multiplicity we find

$$N_{(m)}(Y) \equiv M_{1(m)}^{\text{UTM}}(Y)$$

$$\approx \frac{1}{(m-1)!} \left( -\frac{d}{d\alpha} \right)^{m-1} \left[ \frac{e^{\frac{\alpha}{\gamma}e^{-\Delta Y}}}{\alpha\gamma} \left( \Gamma\left(0, \frac{\alpha}{\gamma}e^{-\Delta Y}\right) + (m-1)\gamma e^{-\frac{\alpha}{\gamma}e^{\Delta Y}} \exp((m-1)\gamma) \right) \right] \Big|_{\alpha=1}$$

$$(4.13)$$

At small Y, the multiplicity  $N_{(m)}(Y)$  from eq. (4.13) tends to the BFKL cascade value  $m e^{\Delta Y}$ . At large Y eq. (4.13) asymptotically gives  $N_{(m)}(Y) \to \frac{\Delta}{\gamma} Y - \frac{1}{\gamma} \ln \frac{1}{\gamma}$ . To reproduce the weak logarithmic dependence on m of eq. (4.12) one would need to keep sub asymptotic terms in the expansion of the incomplete gamma function. At very large Y these corrections are unimportant and we recover the same m-independent asymptotics as given by  $Z_Y^{\text{asymp}}(u)$  eq. (2.38).

# 4.3 UTM at asymptotically large rapidities

If m is not large parametrically, the exact value of m is not very important for the probability distribution in the saturation regime. The onset of the saturation regime is a little

earlier than for m=1, as follows from eq. (4.12), but the distribution itself is practically the same. However if m is very large, i.e.  $m \sim 1/\gamma$  the saturation corrections in the evolution kick in right away. In this case there is no BK or intermediate regime in the evolution and already at low rapidity one can approximate the evolution by eq. (2.37). The solution at arbitrary rapidity then has the form

$$Z_{Y(m)}^{UTM}(u) = e^{\frac{\Delta}{\gamma}(u-1)Y}u^m \tag{4.14}$$

The ensuing dipole distribution is Poisson shifted by the initial number of dipoles

$$P_n^{(m)}(Y) = \frac{\left(\frac{\Delta}{\gamma}Y\right)^{(n-m)}}{(n-m)!}e^{-\frac{\Delta}{\gamma}Y}$$
(4.15)

The mean multiplicity in this cascade

$$N_{(m)} = \frac{\Delta}{\gamma} Y + m \tag{4.16}$$

The influence of the initial number of dipoles m is illustrated by figure 9 where we plot the value of  $N_{(m)}$ . In this figure the two limiting cases are also shown: the value of  $N_{(m)}$  for the BFKL cascade  $N_{(m)} = m \exp{(\Delta Y)}$ , and eq. (4.12), which gives the maximum probability in the saturation region. It is clear from this figure that the transitional region of Y between the BFKL cascade and the asymptotic multiplicity distribution in the saturation region for the UTM cascade shrinks for large m. The values of m that are shown in figure 9, were chosen having in mind m=3 for the "proton", and  $m=3A^{1/3}$  for a "nucleus" of atomic number A.

# 4.4 UTMM — multiple emissions without saturation

We can now repeat the analysis for UTMM. Eq. (A.4) and eq. (A.9) give the factorial moments and  $P_n$  for single dipole initial condition. For the m-dipole case, eq. (3.13) gives  $P_{n < m}^{\text{UTMM}} = 0$ .  $P_m^{\text{UTMM}}$  and  $M_1^{\text{UTMM}}$  are easily determined from this equation, and from eq. (3.15):

$$P_{n < m}^{\text{UTMM}}(Y) = 0; \qquad P_{n = m}^{\text{UTMM}}(Y) = e^{-\Delta Y}; \qquad M_{1(m)}^{\text{UTMM}}(Y) = m e^{\Delta Y}.$$
 (4.17)

The next two moments are determined from eq. (3.17) and eq. (3.19) as:

$$M_{2(m)}^{\text{UTMM}}(Y) = m \frac{(2+\Delta)}{(\Delta+1)} \left( e^{(2+\Delta)\Delta Y} - e^{\Delta Y} \right) + m (m-1) e^{(2+\Delta)\Delta Y}$$

$$\xrightarrow{\Delta \ll 1} 2m \left( e^{\Delta_2 Y} - e^{\Delta_1 Y} \right) + m (m-1) e^{\Delta_2 Y}$$
(4.18)

$$M_{3(m)}^{\text{UTMM}}(Y) = 6 e^{\Delta_3 Y} \int_0^Y dY' e^{-\Delta_3 Y'} M_2(Y') + m(m-1)(m-2) e^{\Delta_3 Y}$$

$$= 3! m \left( e^{\Delta_3 Y} - 2 e^{\Delta_2 Y} + e^{\Delta Y} \right) + 3! m(m-1) \left( e^{\Delta_3 Y} - e^{\Delta_2 Y} \right)$$

$$+ m(m-1)(m-2) e^{\Delta_3 Y}$$

$$(4.19)$$

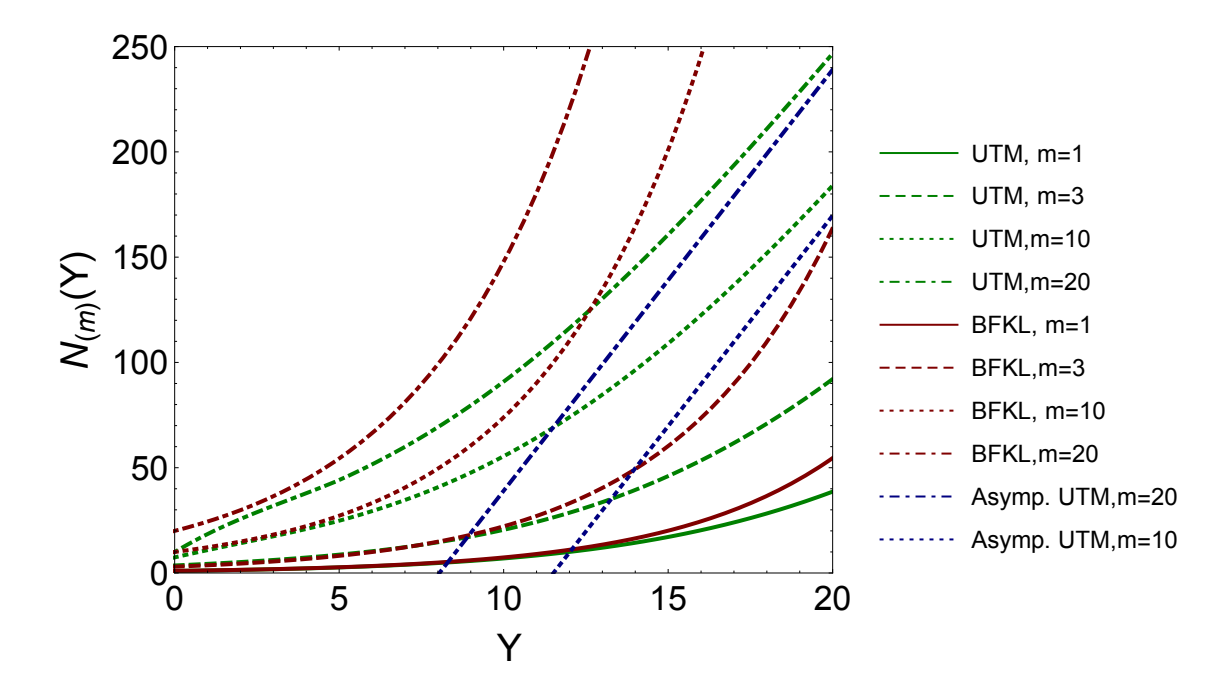


**Figure 9.** The value of  $N_{(m)}$  from eq. (4.13) versus Y. In red it is shown the value for the BFKL cascade (see eq. (4.6)) while in blue the values of  $n_{\text{max}}$  from eq. (4.12) are indicated.

where, as before  $\Delta_k = (1 + \Delta)^k - 1$ . For  $M_{4(m)}^{\text{UTMM}}$  we get:

$$\begin{split} M_{4(m)}^{\text{UTMM}}(Y) &= 12e^{\Delta_4 Y} \int_0^Y dY' e^{-\Delta_4 Y'} M_3(Y') + m(m-1)(m-2)(m-3)e^{\Delta_4 Y} \\ &= 4! m \bigg( e^{\Delta_4 Y} - 3e^{\Delta_3 Y} + 3e^{\Delta_2 Y} - e^{\Delta_1 Y} \bigg) + m(m-1)4! \frac{3}{2} \bigg( e^{\Delta_4 Y} - 2e^{\Delta_3 Y} + e^{\Delta_2 Y} \bigg) \\ &+ 4! \frac{1}{2} m(m-1)(m-2) \bigg( e^{\Delta_4 Y} - e^{\Delta_3 Y} \bigg) + m(m-1)(m-2)(m-3)e^{\Delta_4 Y} \end{split} \tag{4.20}$$

These expressions look rather complicated. However at large rapidities the coefficient of the leading exponent in the k-th moment is easy to determine. We note that at small Y the solution should reduce to that of the BFKL cascade, since multiple emissions are unimportant for small Y. Since the structure of the moments in both regimes is a linear combination of exponentials, when setting  $\Delta_k = k \Delta$ , the moments for UTMM without saturation should reduce to the BFKL moments. This allows us to calculate the combinatorial factor in  $M_{k(m)}^{\text{UTMM}}$  by using the result of the BFKL cascade eq. (4.8b):

$$M_{k(m)}^{\text{UTMM}} \approx \frac{(m+k-1)!}{(m-1)!} e^{\Delta_k Y}.$$
 (4.21)

One can check directly that this reproduces the coefficient of the highest exponent in eq. (4.18), eq. (4.19) and eq. (4.20). Using this expression for the moments we can write

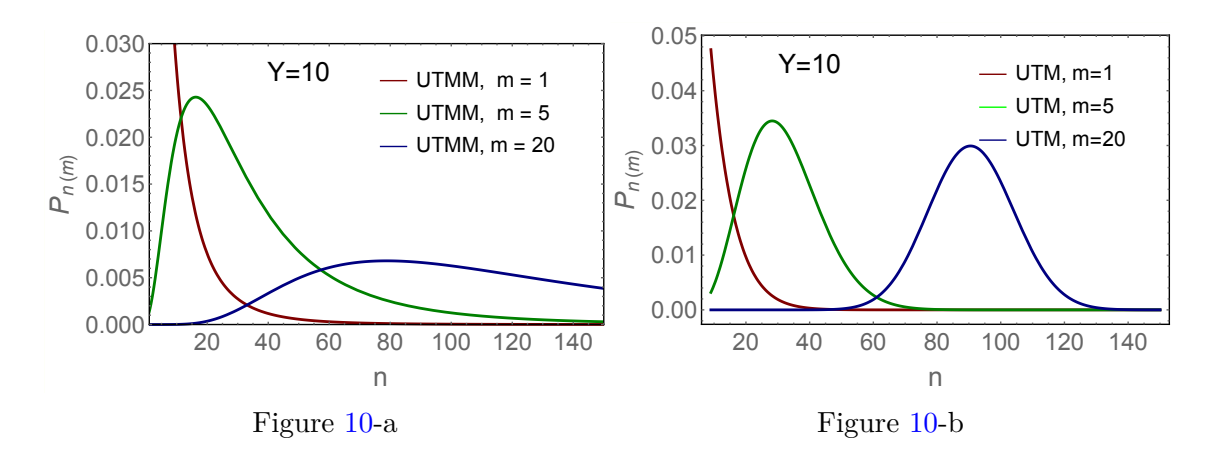


**Figure 10.** Figure 10-a:  $P_n$  from eq. (4.24) (UTMM cascade) versus n at different values of m. Figure 10-b:  $P_n$  for the UTM cascade.  $\Delta = 0.2, \ \gamma = 0.01$ .

the generating function as

$$Z_Y^{\text{UTMM}}(u;m) = 1 + \sum_{k=1}^{\infty} \frac{(m+k-1)!}{(m-1)! \, k!} (u-1)^k e^{\Delta_k Y}. \tag{4.22}$$

We now expand this equation with respect to  $(1 + \Delta)^k Y$ :

$$Z_Y^{\text{UTMM}}(u;m) = e^{-Y} \sum_{j=0}^{\infty} \sum_{k=0}^{\infty} \frac{(m+k-1)!}{(m-1)! \, k!} \frac{(1+\Delta)^{kj} \, Y^j}{j!} (u-1)^k$$
$$= e^{-Y} \sum_{j=0}^{\infty} \frac{Y^j}{j!} \left( \frac{1}{1-(1+\Delta)^j \, (u-1)} \right)^m \tag{4.23}$$

Reexpanding this in powers of  $u^n$ , we obtain the following representation for the probability distribution  $P_n^{\text{UTMM}}(Y)$ :

$$P_n^{\text{UTMM}}(Y) = e^{-Y} \sum_{j=0}^{\infty} \frac{Y^j}{j!} P_n^j \quad \text{with} \quad P_n^j = \frac{(m+n-1)!}{(m-1)! \, n!} \left( \frac{1}{(N_j+1)^m} \left( 1 + \frac{1}{N_j} \right)^{-n} \right)$$
(4.24)

where  $N_i = (1 + \Delta)^j$ .

The multiplicity distribution for eq. (4.24) is plotted in figure 10 at different values of m for Y = 10.

#### 4.5 UTMM with saturation

Finally, when m is large the large Y of UTMM is modified similarly to UTM. In particular the generating function of eq. (3.36) is modified as

$$Z_{\text{asymp}}^{\text{UTMM}} = \exp\left(\left(e^{\frac{\Delta}{\gamma}(u-1)} - 1\right)Y\right)u^m$$
 (4.25)

and the probability distribution is shifted by m

$$P_{n(m)}^{UTMM}(Y) = P_{n-m(1)}^{UTMM}(Y). (4.26)$$

# 5 Discussion

This paper has one central point. For large number of partons in hadronic wave function, rapidity evolution should not be limited by emission of a single parton in one step. Instead many partons can be independently emitted. Here in the framework of a toy model in zero transverse dimensions we have implemented this idea by constructing an evolution which describes independent emission of multiple partons (dipoles). This evolution by construction preserves t-channel and s-channel unitarity. It incorporates saturation dynamics, and reduces to the known simpler models whenever multiple emissions are unimportant. The model has two parameters: the dipole emission probability  $\Delta$ , and dipole-dipole elastic scattering amplitude  $\gamma$ . Within the model itself these parameters are independent, but when projected on QCD we expect  $\Delta \sim \alpha_s$  and  $\gamma \sim \alpha_s^2$ .

In this sense this is an appropriate evolution to be applied for scattering of dense objects, unlike the models of similar type considered so far. We have studied various aspects of probability distributions generated by this evolution from two type of initial conditions: a single dipole and multiple dipoles. An interesting feature of the model worth noting is that the regime where multiple scatterings are important precedes the onset of saturation corrections. Parametrically, as long as the average number of dipole is small  $N < 1/\Delta \sim 1/\alpha_s$ , the single dipole emission dominates the evolution and the probability distribution is that of the BFKL cascade. For intermediate values of N such that  $1/\Delta < N < 1/\gamma$  saturation effects are still unimportant, but multiple dipole emissions are dominant. Finally at very large rapidities where  $N > 1/\gamma$  both, multiple emissions and saturation corrections determine the asymptotic dipole distribution.

There are significant differences between the asymptotic behavior of multiplicity distributions in the model that allows only emission of a single dipole (UTM) and that with multiple dipole emission (UTMM). The main qualitative difference as illustrated on figure 8, is that the distribution in UTMM is significantly wider, and is well approximated by the normal distribution whereas in UTM the asymptotic distribution is of the Poisson type. One can understand this feature directly from the asymptotic form of the generating function Z. Interestingly, in both models the asymptotic distribution can be written in the form

$$Z_Y(u) = (z(u))^Y (5.1)$$

with

$$z_{UTM}(u) = e^{\frac{\Delta}{\gamma}(u-1)} \qquad z_{UTMM}(u) = e^{\left[e^{\frac{\Delta}{\gamma}(u-1)} - 1\right]} = \sum_{k=0}^{\infty} \frac{1}{k!} (z_{UTM} - 1)^k \qquad (5.2)$$

Our discussion in the previous section makes it clear that taking a power m of a distribution function is equivalent to considering a state that evolves into m independent cascades, so that the final probability distribution is that of m cascades. From this point of view the rapidity Y in eq. (5.1) plays the role of the number of independent cascades in the asymptotic distribution.

It is therefore natural to interpret the asymptotic probability distribution in the following way. At pre asymptotic rapidities  $Y < Y_{\text{asymp}}$  an initial state evolves into some fundamental distribution, or cascade z. Starting from  $Y_{\rm asymp}$  the asymptotic evolution takes over, which amounts simply to multiplication of the number of these independent fundamental cascades at a constant rate. At any rapidity  $Y\gg Y_{\rm asymp}$  the number of such fundamental cascades is  $m\approx Y$ . Different evolution dynamics correspond to different properties of the fundamental cascade z eq. (5.2). In UTM  $z_{UTM}$  is a Poisson distribution with average dipole number  $\langle n\rangle = \frac{\Delta}{\gamma}$ . A composition of Y independent Poisson distributions gives again a Poisson distribution with the additive mean value  $N(Y) = \langle n\rangle Y$ , which is precisely what we have seen in section 2. On the other hand in UTMM, since the pre asymptotic evolution is dominated by multiple dipole emission, the fundamental distribution  $z_{UTMM}$  is not a Poisson, but rather a weighted sum of Poisson distributions with averages which are multiples of  $\langle n\rangle$ . A large number of such cascades is not a Poisson distribution anymore. On the other hand we expect that a composition of a large number of identical distributions must lead to a normal distribution, which explains why the distribution on figure 8 is so close to a normal distribution.

In general we saw that including the saturation effects changes the shape of the distribution significantly. In particular while the BK distribution at large Y satisfies KNO scaling, the asymptotic UTM distribution does not. The KNO property is interesting in relation to the recent discussions of parton entropy pioneered in ref. [80]. It was noted in [80] that at large average multiplicities N the entropy of the BFKL cascade behaves as

$$S = \ln N. \tag{5.3}$$

Such behavior can be interpreted in terms of a large number of partonic micro-states having equal probabilities. The proton then is thought of as composed of an exponentially large (in rapidity) number N of micro-states that occur with equal and small probabilities 1/N. More generally one can see that any probability distribution that follows KNO scaling  $P_n = \frac{1}{N}\Psi\left(\frac{n}{N}\right)$ , yields logarithmic entropy

$$S = -\sum_{n} P_n \ln P_n \approx -\int \frac{dn}{N} \Psi\left(\frac{n}{N}\right) \left[-\ln N + \ln \Psi\left(\frac{n}{N}\right)\right] = \ln(aN)$$
 (5.4)

where a is a rapidity independent constant. Strictly speaking, of course not any KNO-type distribution corresponds to equally populated micro states, but physically the situation is not too different. As N grows, KNO scaling means that more and more states (wider range of n's) get populated, if not exactly equally at least according to some fixed probability ratio determined by the KNO function  $\Psi$ . This is the origin of the logarithmic term in the entropy.

In this paper we demonstrated that both the cascade with saturation, and a possibility to emit many partons lead to violations of KNO scaling. It would be interesting to see to what extent this also leads to violation of eq. (5.3). We can answer this question for asymptotic rapidities. Both in UTM and UTMM at very large rapidities the distribution is well approximated by normal distribution with  $\sigma^2 \propto N$ . Estimate similar to eq. (5.4) then gives

$$S = \ln a\sigma = \frac{1}{2}\ln N + const \tag{5.5}$$

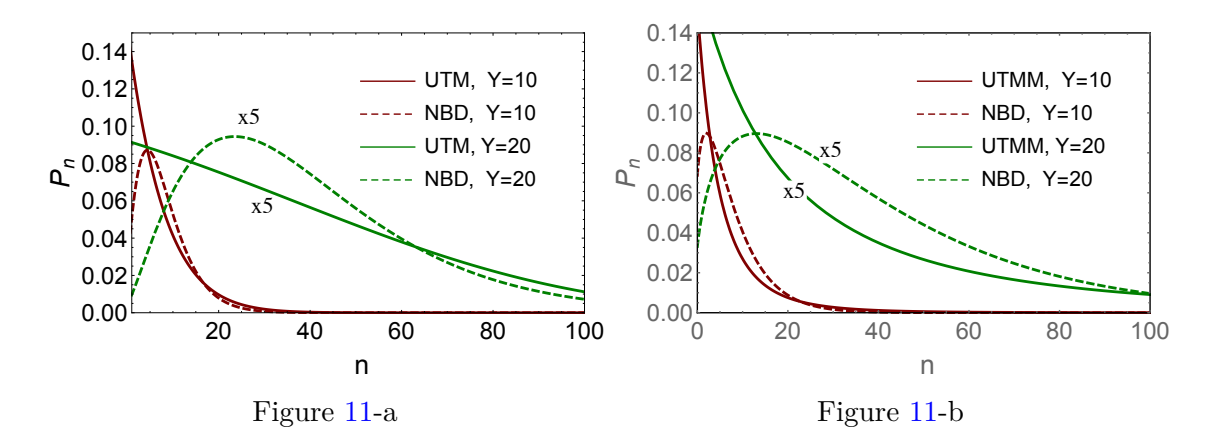


Figure 11. Comparison between multiplicity distributions in UTM and UTMM cascade with the negative binomial distributions which have the same  $M_1$  and  $M_2$  as the cascades. At the plots,  $P_n$  are multiplied by 5 for Y=20, to fit the scale.  $\Delta = 0.2, \gamma = 0.01$ .

This differs from eq. (5.3) by a factor of two, which reflects the difference scaling property of the distribution with N.

The second point we want to stress is that at intermediate rapidities the distribution with saturation is poorly described by the negative binomial distribution of eq. (3.45), see figure 11. Within the CGC approach the multiplicity distribution was calculated in the MV model, the so called "glittering glasma" [81, 82]. This leads to NBD in which the average number of partons and parameter r are determined by the first and the second factorial moments. Both UTM and UTMM are far from NBD at intermediate rapidities, although interestingly in the asymptotic regime the UTMM cascade is quantitatively not very different from NBD figure 8-d.

We believe the main point of this paper is valid beyond the toy model and generalizes to high energy scattering in QCD as well. The BK regime in QCD should not transition directly into the saturation regime as far as the evolution of the wave function is concerned. Rather the saturation should be preceded by the rapidity range where multiple gluon emissions in the evolution play prominent role. The study of this new regime is an interesting problem which should start by the derivation of the generalization of the BK Hamiltonian.

# Acknowledgments

We thank our colleagues at Tel Aviv university and UTFSM for encouraging discussions. AK was supported by the NSF Nuclear Theory grant 1913890. EL was supported by ANID PIA/APOYO AFB180002 (Chile), Fondecyt grant #1180118 (Chile) and the Tel Aviv university encouragement grant #5731. ML and AK were supported by the Binational Science Foundation grant #2018722, and the Horizon 2020 RISE "Heavy ion collisions: collectivity and precision in saturation physics" under grant agreement No. 824093.

# A Factorial moments and probabilities in UTMM

Here we derive the approximate result for the factorial moments of the distribution which generalizes eq. (3.21).

Using  $M_k^{\text{UTMM}} = \frac{d^k}{du^k} Z_Y^{\text{UTMM}}(u)|_{u=1}$  and the Schroedinger equation eq. (3.14) we obtain the equation for the factorial moments

$$\frac{dM_k^{\text{UTMM}}(Y)}{dY} = \frac{d}{dY} \frac{d^k}{du^k} Z_Y^{\text{UTMM}}(u)|_{u=1} = \left(\frac{d^k}{du^k} \sum_{n=1}^{\infty} \Delta^n (u-1)^n \left(u \frac{d}{du}\right)^n Z_Y^{\text{UTMM}}(u)\right)\Big|_{u=1} \\
= \left(\frac{d^k}{du^k} \sum_{n=1}^k \Delta^n (u-1)^n \left(u \frac{d}{du}\right)^n Z_Y^{\text{UTMM}}(u)\right)\Big|_{u=1} \tag{A.1}$$

With some arduous algebra the right hand side of this equation can be rewritten in terms of the moments  $M_m^{\rm UTMM}$ . This expression is a linear function of all  $M_j^{\rm UTMM}$  with  $j \leq k$ . We know however that at small  $\Delta$  and large rapidity the higher moments are exponentially larger than the lower ones. Thus at high rapidity we do not need to keep all the terms in the r.h.s. The largest term is the one that is proportional to  $M_k^{\rm UTMM}$ . Keeping only this term would give us a homogeneous equation for  $M_k^{\rm UTMM}$ , and although we would be able to determine the largest term at high Y, we would not be able to impose the correct initial condition. We therefore also keep the next largest term which contributes to the non homogeneous term in eq. (A.1). We will however disregard perturbative in  $\Delta$  corrections to the prefactors in the exponentials. This makes it possible to simplify eq. (A.1) by substituting  $u\frac{d}{du} \to \frac{d}{du}$  in all but n=1 terms

$$\frac{d M_k^{\text{UTMM}}(Y)}{d Y} \approx \left( \frac{d^k}{d u^k} \left( \Delta (u - 1) u \frac{d}{d u} + \sum_{n=2}^k \Delta^n (u - 1)^n \left( \frac{d}{d u} \right)^n \right) Z_Y^{\text{UTMM}}(t) \right) \Big|_{u=1}$$

$$= \Delta_k M_k^{\text{UTMM}}(Y) + \Delta k (k - 1) M_{k-1}^{\text{UTMM}}(Y) \tag{A.2}$$

where  $\Delta_k = (1+\Delta)^k - 1$ . The solution to eq. (A.2) with a single dipole initial condition is:

$$M_k^{\text{UTMM}}(Y) = \Delta k(k-1) e^{\Delta_k Y} \int_0^Y dY' M_{k-1}^{\text{UTMM}} (Y') e^{-\Delta_k Y'}$$
 (A.3)

Note, that eq. (A.3) determines  $M_k^{\text{UTMM}}$  for  $k \geq 2$  while for  $M_1^{\text{UTMM}}$  we have the solution of eq. (3.16).

Inspired by eq. (3.18) and eq. (3.21) we make the induction hypothesis, that  $M_j^{\text{UTMM}}$  for  $j \leq k-1$  has the form:

$$M_j^{\text{UTMM}}(Y) = j! \left( \sum_{l=0}^{j-1} (-1)^l \frac{(j-1)!}{(j-1-l)! \, l!} e^{\Delta_{j-l} Y} \right)$$
(A.4)

Substituting this into eq. (A.3) we now prove eq. (A.4) for  $M_k^{\text{UTMM}}(Y)$ . Substitution of eq. (A.4) into eq. (A.3) yields:

$$M_{k}^{\text{UTMM}}(Y) = k! \left( \underbrace{\sum_{l=0}^{k-2} \frac{(-1)^{l}(k-1)!}{(k-2-l)! \, l!} \frac{\Delta}{\Delta_{k} - \Delta_{l+1}}}_{= 1} \right) e^{\Delta_{k} Y}$$

$$+ \sum_{l=0}^{k-2} \frac{(-1)^{k-l}(k-1)!}{(k-2-l)! \, l!} \frac{\Delta}{\Delta_{k} - \Delta_{l+1}} e^{\Delta_{k-l}, Y} \right)$$

$$\approx k! \left( \sum_{l=0}^{k-1} (-1)^{l} \frac{(k-1)!}{(k-1-l)! \, l!} e^{\Delta_{k-l} Y} \right)$$
(A.5a)

To obtain the second line we have used  $\Delta_k - \Delta_l \approx (k-l)\Delta$  and changed the summation index from l to l+1. Within our approximation we are allowed to use the small  $\Delta$  limit in the prefactor of each exponent on the right hand side of eq. (A.5b) while keeping the complete expression for  $\Delta_k$  in the exponent. We now see that eq. (A.5b) coincides with eq. (A.4). Bearing in mind eqs. (3.15)–(3.21), we conclude that eq. (A.4) is valid for all k.

We next derive approximate expressions for probabilities at large rapidity Y. Using eq. (A.4) we can calculate the generating function  $Z^{\text{UTMM}}(u)$ , since

$$Z_Y^{\text{UTMM}}(u) = 1 + \sum_{k=1}^{\infty} \frac{M_k^{\text{UTMM}}(Y)}{k!} (u-1)^k$$
 (A.6)

We take the simplified expression at large Y:  $M_k^{\text{UTMM}} = k! e^{\Delta_k Y}$  (see eq. (A.5b)). Then

$$Z_Y^{\text{UTMM}}(u) = 1 + \sum_{k=1}^{\infty} e^{\Delta_k Y} (u - 1)^k$$
 (A.7)

Since  $\Delta_k = (1 + \Delta)^k - 1$ , the series of eq. (A.7) is divergent. To sum such an asymptotic series we need to invent analytical function, which has the same series. We suggest the following procedure: plugging in eq. (A.7)  $\Delta_k$  we can expand with respect to parameter  $(1 + \Delta)^k Y$ : viz.:

$$Z_Y^{\text{UTMM}}(u) = e^{-Y} \sum_{j=0}^{\infty} \sum_{k=0}^{\infty} \frac{(1+\Delta)^{kj} Y^j}{j!} (u-1)^k = e^{-Y} \sum_{j=0}^{\infty} \frac{Y^j}{j!} \frac{1}{1-(1+\Delta)^j (u-1)}$$
(A.8)

Expending eq. (A.8) with respect to  $u^n$ , we obtain the following expression for  $P_n^{\text{UTMM}}(Y)$ :

$$P_{n}^{\text{UTMM}}(Y) = e^{-Y} \sum_{j=0}^{\infty} \frac{Y^{j}}{j!} P_{n}^{j} \quad \text{with} \quad P_{n}^{j} = \frac{1}{N_{j}} \left( 1 + \frac{1}{N_{j}} \right)^{-n} \xrightarrow{N_{j} > 1, n > 1} \frac{1}{N_{j}} \exp\left( -\frac{n}{N_{j}} \right) \tag{A.9}$$

where  $N_i = (1 + \Delta)^j$ .

Since we have made some approximations, it is instructive to check that eq. (A.9) leads to the factorial moments  $M_k^{\text{UTMM}} \xrightarrow{Y \gg 1} < |n^k| > = k! \exp{(\Delta_k Y)}$ , reproducing eq. (A.7).

**Open Access.** This article is distributed under the terms of the Creative Commons Attribution License (CC-BY 4.0), which permits any use, distribution and reproduction in any medium, provided the original author(s) and source are credited.

# References

- [1] V.S. Fadin, E.A. Kuraev and L.N. Lipatov, On the Pomeranchuk singularity in asymptotically free theories, Phys. Lett. B 60 (1975) 50 [INSPIRE].
- [2] E.A. Kuraev, L.N. Lipatov and V.S. Fadin, The Pomeranchuk singularity in nonabelian gauge theories, Sov. Phys. JETP 45 (1977) 199 [Zh. Eksp. Teor. Fiz. 72 (1977) 377] [INSPIRE].
- [3] I.I. Balitsky and L.N. Lipatov, The Pomeranchuk singularity in quantum chromodynamics, Sov. J. Nucl. Phys. 28 (1978) 822 [Yad. Fiz. 28 (1978) 1597] [INSPIRE].
- [4] L.N. Lipatov, The bare Pomeron in quantum chromodynamics, Sov. Phys. JETP 63 (1986) 904 [Zh. Eksp. Teor. Fiz. 90 (1986) 1536] [INSPIRE].
- [5] L.V. Gribov, E.M. Levin and M.G. Ryskin, Semihard processes in QCD, Phys. Rept. 100 (1983) 1 [INSPIRE].
- [6] A.H. Mueller and J.-W. Qiu, Gluon recombination and shadowing at small values of x, Nucl. Phys. B 268 (1986) 427 [INSPIRE].
- [7] A.H. Mueller and B. Patel, Single and double BFKL Pomeron exchange and a dipole picture of high-energy hard processes, Nucl. Phys. B 425 (1994) 471 [hep-ph/9403256] [INSPIRE].
- [8] A.H. Mueller, Soft gluons in the infinite momentum wave function and the BFKL Pomeron, Nucl. Phys. B 415 (1994) 373 [INSPIRE].
- [9] A.H. Mueller, Unitarity and the BFKL Pomeron, Nucl. Phys. B 437 (1995) 107
   [hep-ph/9408245] [INSPIRE].
- [10] L.N. Lipatov, Small x physics in perturbative QCD, Phys. Rept. 286 (1997) 131 [hep-ph/9610276] [INSPIRE].
- [11] L.N. Lipatov, High-energy scattering in QCD and in quantum gravity and two-dimensional field theories, Nucl. Phys. B 365 (1991) 614 [INSPIRE].
- [12] L.N. Lipatov, Gauge invariant effective action for high-energy processes in QCD, Nucl. Phys. B 452 (1995) 369 [hep-ph/9502308] [INSPIRE].
- [13] R. Kirschner, L.N. Lipatov and L. Szymanowski, Effective action for multi-Regge processes in QCD, Nucl. Phys. B 425 (1994) 579 [hep-th/9402010] [INSPIRE].
- [14] R. Kirschner, L.N. Lipatov and L. Szymanowski, Symmetry properties of the effective action for high-energy scattering in QCD, Phys. Rev. D 51 (1995) 838 [hep-th/9403082] [INSPIRE].
- [15] J. Bartels, Unitarity corrections to the Lipatov Pomeron and the four gluon operator in deep inelastic scattering in QCD, Z. Phys. C 60 (1993) 471 [INSPIRE].
- [16] J. Bartels and M. Wusthoff, The triple Regge limit of diffractive dissociation in deep inelastic scattering, Z. Phys. C 66 (1995) 157 [INSPIRE].
- [17] J. Bartels and C. Ewerz, *Unitarity corrections in high-energy QCD*, *JHEP* **09** (1999) 026 [hep-ph/9908454] [INSPIRE].
- [18] C. Ewerz, Reggeization in high-energy QCD, JHEP 04 (2001) 031 [hep-ph/0103260] [INSPIRE].

- [19] J. Bartels, High-energy behavior in a non-Abelian gauge theory (II): first corrections to  $T_{n\to m}$  beyond the leading ln s approximation, Nucl. Phys. B 175 (1980) 365 [INSPIRE].
- [20] J. Kwiecinski and M. Praszalowicz, Three gluon integral equation and odd c singlet Regge singularities in QCD, Phys. Lett. B 94 (1980) 413 [INSPIRE].
- [21] L.D. McLerran and R. Venugopalan, Computing quark and gluon distribution functions for very large nuclei, Phys. Rev. D 49 (1994) 2233 [hep-ph/9309289] [INSPIRE].
- [22] L.D. McLerran and R. Venugopalan, Gluon distribution functions for very large nuclei at small transverse momentum, Phys. Rev. D 49 (1994) 3352 [hep-ph/9311205] [INSPIRE].
- [23] A.H. Mueller and G.P. Salam, Large multiplicity fluctuations and saturation effects in onium collisions, Nucl. Phys. B 475 (1996) 293 [hep-ph/9605302] [INSPIRE].
- [24] G.P. Salam, Studies of unitarity at small x using the dipole formulation, Nucl. Phys. B **461** (1996) 512 [hep-ph/9509353] [INSPIRE].
- [25] Y.V. Kovchegov and E. Levin, Diffractive dissociation including multiple Pomeron exchanges in high parton density QCD, Nucl. Phys. B 577 (2000) 221 [hep-ph/9911523] [INSPIRE].
- [26] M. Braun, Structure function of the nucleus in the perturbative QCD with  $N_c \to \infty$  (BFKL Pomeron fan diagrams), Eur. Phys. J. C 16 (2000) 337 [hep-ph/0001268] [INSPIRE].
- [27] M.A. Braun and G.P. Vacca, Triple Pomeron vertex in the limit  $N_c \to \infty$ , Eur. Phys. J. C 6 (1999) 147 [hep-ph/9711486] [INSPIRE].
- [28] J. Bartels, M. Braun and G.P. Vacca, Pomeron vertices in perturbative QCD in diffractive scattering, Eur. Phys. J. C 40 (2005) 419 [hep-ph/0412218] [INSPIRE].
- [29] J. Bartels, L.N. Lipatov and G.P. Vacca, Interactions of reggeized gluons in the Mobius representation, Nucl. Phys. B 706 (2005) 391 [hep-ph/0404110] [INSPIRE].
- [30] M.A. Braun, Nucleus-nucleus scattering in perturbative QCD with  $N_c \to \infty$ , Phys. Lett. B 483 (2000) 115 [hep-ph/0003004] [INSPIRE].
- [31] M.A. Braun, Nucleus nucleus interaction in the perturbative QCD, Eur. Phys. J. C 33 (2004) 113 [hep-ph/0309293] [INSPIRE].
- [32] M.A. Braun, Conformal invariant Pomeron interaction in the perurbative QCD with large  $N_c$ , Phys. Lett. B 632 (2006) 297 [hep-ph/0512057] [INSPIRE].
- [33] I. Balitsky, Factorization and high-energy effective action, Phys. Rev. D **60** (1999) 014020 [hep-ph/9812311] [INSPIRE].
- [34] Y.V. Kovchegov, Small x F<sub>2</sub> structure function of a nucleus including multiple Pomeron exchanges, Phys. Rev. D **60** (1999) 034008 [hep-ph/9901281] [INSPIRE].
- [35] T. Altinoluk, A. Kovner, E. Levin and M. Lublinsky, Reggeon field theory for large Pomeron loops, JHEP 04 (2014) 075 [arXiv:1401.7431] [INSPIRE].
- [36] A. Kovner and M. Lublinsky, In pursuit of Pomeron loops: the JIMWLK equation and the Wess-Zumino term, Phys. Rev. D 71 (2005) 085004 [hep-ph/0501198] [INSPIRE].
- [37] A. Kovner and M. Lublinsky, From target to projectile and back again: selfduality of high energy evolution, Phys. Rev. Lett. 94 (2005) 181603 [hep-ph/0502119] [INSPIRE].
- [38] Y. Hatta, E. Iancu, L. McLerran, A. Stasto and D.N. Triantafyllopoulos, *Effective Hamiltonian for QCD evolution at high energy*, *Nucl. Phys. A* **764** (2006) 423 [hep-ph/0504182] [INSPIRE].

- [39] A. Kovner, M. Lublinsky and U. Wiedemann, From bubbles to foam: dilute to dense evolution of hadronic wave function at high energy, JHEP 06 (2007) 075 [arXiv:0705.1713] [INSPIRE].
- [40] T. Altinoluk, A. Kovner, M. Lublinsky and J. Peressutti, QCD Reggeon field theory for every day: Pomeron loops included, JHEP 03 (2009) 109 [arXiv:0901.2559] [INSPIRE].
- [41] A.H. Mueller and A.I. Shoshi, Small x physics beyond the Kovchegov equation, Nucl. Phys. B 692 (2004) 175 [hep-ph/0402193] [INSPIRE].
- [42] E. Iancu and D.N. Triantafyllopoulos, A Langevin equation for high energy evolution with Pomeron loops, Nucl. Phys. A **756** (2005) 419 [hep-ph/0411405] [INSPIRE].
- [43] E. Iancu and D.N. Triantafyllopoulos, Non-linear QCD evolution with improved triple-Pomeron vertices, Phys. Lett. B 610 (2005) 253 [hep-ph/0501193] [INSPIRE].
- [44] E. Iancu, G. Soyez and D.N. Triantafyllopoulos, On the probabilistic interpretation of the evolution equations with Pomeron loops in QCD, Nucl. Phys. A 768 (2006) 194 [hep-ph/0510094] [INSPIRE].
- [45] A.H. Mueller, A.I. Shoshi and S.M.H. Wong, Extension of the JIMWLK equation in the low gluon density region, Nucl. Phys. B 715 (2005) 440 [hep-ph/0501088] [INSPIRE].
- [46] E. Levin and M. Lublinsky, Balitsky's hierarchy from Mueller's dipole model and more about target correlations, Phys. Lett. B 607 (2005) 131 [hep-ph/0411121] [INSPIRE].
- [47] E. Levin and M. Lublinsky, Towards a symmetric approach to high energy evolution: generating functional with Pomeron loops, Nucl. Phys. A 763 (2005) 172 [hep-ph/0501173] [INSPIRE].
- [48] A. Kormilitzin, E. Levin and A. Prygarin, Multiparticle production in the mean field approximation of high density QCD, Nucl. Phys. A 813 (2008) 1 [arXiv:0807.3413] [INSPIRE].
- [49] E. Levin, J. Miller and A. Prygarin, Summing Pomeron loops in the dipole approach, Nucl. Phys. A 806 (2008) 245 [arXiv:0706.2944] [INSPIRE].
- [50] E. Levin, Dipole-dipole scattering in CGC/saturation approach at high energy: summing Pomeron loops, JHEP 11 (2013) 039 [arXiv:1308.5052] [INSPIRE].
- [51] J. Jalilian-Marian, A. Kovner, A. Leonidov and H. Weigert, *The BFKL equation from the Wilson renormalization group, Nucl. Phys. B* **504** (1997) 415 [hep-ph/9701284] [INSPIRE].
- [52] J. Jalilian-Marian, A. Kovner, A. Leonidov and H. Weigert, *The Wilson renormalization group for low x physics: towards the high density regime*, *Phys. Rev. D* **59** (1998) 014014 [hep-ph/9706377] [INSPIRE].
- [53] A. Kovner, J.G. Milhano and H. Weigert, Relating different approaches to nonlinear QCD evolution at finite gluon density, Phys. Rev. D 62 (2000) 114005 [hep-ph/0004014] [INSPIRE].
- [54] E. Iancu, A. Leonidov and L.D. McLerran, Nonlinear gluon evolution in the color glass condensate. 1, Nucl. Phys. A 692 (2001) 583 [hep-ph/0011241] [INSPIRE].
- [55] E. Iancu, A. Leonidov and L.D. McLerran, *The renormalization group equation for the color glass condensate*, *Phys. Lett. B* **510** (2001) 133 [hep-ph/0102009] [INSPIRE].
- [56] E. Ferreiro, E. Iancu, A. Leonidov and L. McLerran, Nonlinear gluon evolution in the color glass condensate. 2, Nucl. Phys. A 703 (2002) 489 [hep-ph/0109115] [INSPIRE].
- [57] H. Weigert, Unitarity at small Bjorken x, Nucl. Phys. A 703 (2002) 823 [hep-ph/0004044] [INSPIRE].

- [58] A. Kovner and M. Lublinsky, From target to projectile and back again: selfduality of high energy evolution, Phys. Rev. Lett. **94** (2005) 181603 [hep-ph/0502119] [INSPIRE].
- [59] A. Kovner, E. Levin, M. Li and M. Lublinsky, *The JIMWLK evolution and the s-channel unitarity*, *JHEP* **09** (2020) 199 [arXiv:2006.15126] [INSPIRE].
- [60] A. Kovner, E. Levin, M. Li and M. Lublinsky, Reggeon field theory and self duality: making ends meet, JHEP 10 (2020) 185 [arXiv:2007.12132] [INSPIRE].
- [61] D. Amati, L. Caneschi and R. Jengo, Summing Pomeron trees, Nucl. Phys. B 101 (1975) 397 [INSPIRE].
- [62] V. Alessandrini, D. Amati and R. Jengo, One-dimensional quantum theory of the Pomeron, Nucl. Phys. B 108 (1976) 425 [INSPIRE].
- [63] R. Jengo, Zero slope limit of the Pomeron field theory, Nucl. Phys. B 108 (1976) 447 [INSPIRE].
- [64] D. Amati, M. Le Bellac, G. Marchesini and M. Ciafaloni, Reggeon field theory for  $\alpha(0) > 1$ , Nucl. Phys. B **112** (1976) 107 [INSPIRE].
- [65] M. Ciafaloni, M. Le Bellac and G.C. Rossi, Reggeon quantum mechanics: a critical discussion, Nucl. Phys. B 130 (1977) 388 [INSPIRE].
- [66] M. Ciafaloni, Instanton contributions in Reggeon quantum mechanics, Nucl. Phys. B 146 (1978) 427 [INSPIRE].
- [67] P. Rembiesa and A.M. Stasto, Algebraic models for the hierarchy structure of evolution equations at small x, Nucl. Phys. B 725 (2005) 251 [hep-ph/0503223] [INSPIRE].
- [68] A. Kovner and M. Lublinsky, More remarks on high energy evolution, Nucl. Phys. A 767 (2006) 171 [hep-ph/0510047] [INSPIRE].
- [69] A.I. Shoshi and B.-W. Xiao, Pomeron loops in zero transverse dimensions, Phys. Rev. D 73 (2006) 094014 [hep-ph/0512206] [INSPIRE].
- [70] M. Kozlov and E. Levin, Solution for the BFKL Pomeron calculus in zero transverse dimensions, Nucl. Phys. A 779 (2006) 142 [hep-ph/0604039] [INSPIRE].
- [71] J.-P. Blaizot, E. Iancu and D.N. Triantafyllopoulos, A zero-dimensional model for high-energy scattering in QCD, Nucl. Phys. A 784 (2007) 227 [hep-ph/0606253] [INSPIRE].
- [72] N. Armesto, S. Bondarenko, J.G. Milhano and P. Quiroga, Reaction-diffusion processes in zero transverse dimensions as toy models for high-energy QCD, JHEP 05 (2008) 103 [arXiv:0803.0820] [INSPIRE].
- [73] E. Levin and A. Prygarin, The BFKL Pomeron calculus in zero transverse dimension: summation of the Pomeron loops and the generating functional for the multiparticle production processes, Eur. Phys. J. C 53 (2008) 385 [hep-ph/0701178] [INSPIRE].
- [74] A. Kovner, E. Levin and M. Lublinsky, QCD unitarity constraints on Reggeon field theory, JHEP 08 (2016) 031 [arXiv:1605.03251] [INSPIRE].
- [75] A. Kovner and M. Lublinsky, More remarks on high energy evolution, Nucl. Phys. A 767 (2006) 171 [hep-ph/0510047] [INSPIRE].
- [76] A.M. Polyakov, A similarity hypothesis in the strong interactions. 1. Multiple hadron production in e<sup>+</sup>e<sup>-</sup> annihilation, Sov. Phys. JETP **32** (1971) 296 [Zh. Eksp. Teor. Fiz. **59** (1970) 542] [INSPIRE].

- [77] Z. Koba, H.B. Nielsen and P. Olesen, Scaling of multiplicity distributions in high-energy hadron collisions, Nucl. Phys. B 40 (1972) 317 [INSPIRE].
- [78] Z. Koba, Multi-body phenomena in strong interactions description of hadronic multi-body final states, CERN Yellow Report CERN-73-12, CERN, Geneva, Switzerland (1973), p. 171.
- [79] I. Gradstein and I. Ryzhik, *Table of integrals, series and products*, fifth edition, Academic Press, London, U.K. (1994).
- [80] D.E. Kharzeev and E.M. Levin, *Deep inelastic scattering as a probe of entanglement*, *Phys. Rev. D* **95** (2017) 114008 [arXiv:1702.03489] [INSPIRE].
- [81] F. Gelis, T. Lappi and L. McLerran, Glittering glasmas, Nucl. Phys. A 828 (2009) 149 [arXiv:0905.3234] [INSPIRE].
- [82] A. Dumitru, F. Gelis, L. McLerran and R. Venugopalan, Glasma flux tubes and the near side ridge phenomenon at RHIC, Nucl. Phys. A 810 (2008) 91 [arXiv:0804.3858] [INSPIRE].